The Specialist Committee on Detailed Flow Measurements

Final Report and Recommendations to the 26th ITTC

1. INTRODUCTION

1.1 Membership

The 26th ITTC Specialist Committee on Detailed Flow Measurements consisted of:

- Dr. Paisan Atsavapranee (Chairman)
  Naval Surface Warfare Center Carderock Division (NSWCCD), USA
- Prof. Sandy Day (Secretary)
  University of Glasgow and Strathclyde, UK
- Dr. Mario Felli
  Istituto Nazionale per Studi ed Esperienze di Architettura Navale (NSEAN), Italy
- Prof. Arnold Fontaine
  Pennsylvania State University, USA
- Prof. Takafumi Kawamura
  University of Tokyo, Japan
- Mr. Olivier Perelman
  Bassin d'Essais des Carènes, France
- Mr. Roderick Sampson
  University of Newcastle upon Tyne, UK
- Dr. Feng Zhao
  China Ship Scientific Research Center (CSSRC), China

1.2 Meetings

The committee met four times:

- INSEAN, Italy, February 2009
- Ecole Centrale de Nantes, France, September 2009
- University of Tokyo, Japan, March 2010
- University of Newcastle upon Tyne, UK, April 2011

2. SCOPE

The scope of this report is to review up-to-date measurement systems and methods available for flow-field and wave-field measurements and describe applications of Particle Image Velocimetry (PIV), stereoscopic PIV (SPIV), Laser Doppler Velocimetry (LDV), Particle Tracking Velocimetry (PTV), holography, and other emergent methods, for the measurements of flow separation, wake, vortex strength, etc, for ship hydrodynamics problems. Furthermore, practical issues related to the application of these measurement techniques, especially PIV and SPIV, in large-scale tow tank facilities and cavitation tunnels will be discussed, with recommendations for future work for the ITTC in these areas.

3. OVERVIEW

Detailed flow measurement has played an important role in the understanding of flow physics and the evaluation of hydrodynamic performance of marine vessels and off-shore structures in the last few decades. In recent years, some image-based measurement systems have been used to investigate various problems in ship hydrodynamics in towing tanks and on

full-scale ships. These measurements yield simultaneous multi-point flow quantities (plane or volume) that are particularly suitable for the benchmarking of unsteady computational fluid dynamics (CFD) codes and the development of physics-based models.

It is a common perception that the advent of more sophisticated numerical modelling is the driver of advancement in experimental measurements. The truth in our opinion is that the two go hand-in-hand. Advancement in numerical modelling and computation would not have been possible without the detailed quantitative data from state-of-the-art measurement techniques. Together, the parallel advancement has allowed researchers to investigate more complex hydrodynamic problems, including unsteady and nonlinear phenomena.

Early adoption of single-point laser-based flow measurement techniques such as LDV has its root in the field of propeller hydrodynamics. In order to analyze the performance of the propeller as affected by the presence of the hull, potential and viscous contribution to the wake has to be characterized. Wake survey is central to the performance analysis of the propeller, as non-uniformity of the wake has many undesirable effects. As the blades rotate through the non-uniform wake, periodic forcing on the blades is transmitted through the shaft bearings and to the ship, creating hull vibration. The specific nature of the wake also influences onset of cavitation and the resulting vibration and blade erosion. Early measurements utilized intrusive methods such as pitot tubes and hot-wire anemometry, each with its own limitations but the most significant being the intrusive presence of the probes themselves. With the advent and maturation of the LDV technique and the availability of commercial systems in the early 80's, researchers in this field began to adopt this non-intrusive optical technique. Significant knowledge and understanding on propeller flow, especially regarding the turbulence characteristics, can be attributed to the application of the LDV measurement technique and is today routinely used by research organizations and test tank facilities around the world.

As much as LDV is an improvement over pitot tubes and hot wires, it is not without its own set of limitations. Being an inherently single-point technique, it is unsuitable for the studies of flows involving large unsteady vortical structures. In addition, to obtain the whole field of velocity information, the LDV probe is traversed point-by-point along multiple axes, and the entire process can take a significant amount of facility time. PIV-based flow measurement alleviates most of these concerns and is now finding growing use along with that of LDV.

PIV and its variants (stereo-PIV, PTV, etc) are whole-field instantaneous measurement techniques that yield either two components or three components of velocity in a single plane. Over the past decade, the PIV-based techniques have matured considerably and thus are finding broadening use within the ITTC community. The maturation of PIV is due partially to the improvement in the hardware components, such as high-energy pulse lasers, high-resolution and low-noise CCD cameras, fast frame grabbers, faster computers and cheaper data storage; and partially to improvement to the post-processing algorithms such as advanced cross-correlation techniques and more robust calibration schemes.

Beyond finding a place within LDV's traditional usage space, PIV is allowing researchers to investigate complex flow phenomena that were never before possible. As previously mentioned, the primary advantage of PIV is that it allows whole-field instantaneous measurement of flow velocity, making it uniquely suitable for the study of complex nonlinear flow phenomena, involving large unsteady flow structures. More recently, PIV and SPIV have found use in the investigation of massive cross-flow separation for maneuvering ships and submarines and

complex viscous phenomena associated with large-amplitude ship motions in high sea states.

The "hand-in-hand" relationship between the development of detailed flow measurement and the advancement of state-of-the-art numerical techniques can not be more evident than in the fields of ship maneuvering and seakeeping. Even with the increasing availability of CFD tools, traditional analytical methods such as coefficient-based maneuvering simulations and linear frequency-domain seakeeping codes are still widely used today. Because these traditional analytical tools are based on coefficient or inviscid models, little emphasis has been placed on comparison with measurements of complex viscous flow fields. However, new and more demanding applications involving complex maneuvers and severe ship motions are providing researchers with the impetus to increasingly adopt both CFD tools and advanced flow measurements to study these phenomena.

Similar challenges exist in the measurement of wave elevation and profile, related to ship-generated waves and the interaction of ships and ocean structures with the surrounding environment. Traditional single-point techniques such as resistance, capacitance or servo-mechanical probes are suitable for discrete measurements of relatively small waves at zero or moderate forward speed. However, as interest grows in applications involving complex non-linear phenomena such as steep bow waves, transom wakes from high-speed ships, and survival of ships and ocean structures in large breaking waves, the limitations of traditional techniques need to be addressed. As a consequence, it is increasingly desirable to use non-intrusive techniques which can cope with challenging wave conditions, resulting from large steep waves, high forward speed and white water. Even greater advantages can be gained if wave elevation measurements can be made along a line or over a two-dimensional patch.

This report provides a comprehensive review of the applications of detailed flow measurements in many ship hydrodynamics disciplines in Section 4 and provides a discussion of current and emerging measurement techniques in Section 5. Numerous ITTC committees have previously provided excellent reviews in their respective areas; therefore, this report partly summarizes and supplements those findings and addresses work performed since the 25th conference.

While the reviews as outlined in Section 4 and 5 are the main focus of the Committee as specified by the terms of reference, the Committee has in addition considered various issues that it considers crucial towards wider adoption and application of detailed flow measurements within the ITTC community. The work, as described in Section 6, is preliminary in nature but would hopefully lay the foundation for more focused efforts for the 27th conference:

- The committee has considered practical issues for PIV/SPIV applications in large-scale test facilities.
- The committee has assessed the need for experimental benchmarks for the verification of PIV/SPIV setup.
- The committee has assessed the need for continued development of uncertainty analysis procedures for PIV/SPIV, and the definition of technical standards and certification requirements.
- The committee has recognized the need to evaluate the use of flow measurements in the verification and validation of CFD and advance the process and procedure for such use.

4. STATE-OF-THE-ART REVIEW

4.1 Applications of Detailed Flow Measurements in Ship Propulsion

The use of detailed flow measurements in the ship propulsion community has been comprehensively reviewed by the 21st, 22nd, and 25th ITTC Propulsor Committees. The current review partially summarizes and supplements those findings and also addresses work performed since the 25th conference.

The applications of detailed flow measurements in the propulsion field date back to the late 70's and for many years concerned the use of Laser Doppler Velocimetry (LDV) to quantify complex flow details needed for the validation of prediction tools, such as lifting surface, panel methods and RANS codes. Adoption of Particle Image Velocimetry (PIV) in the late 90's has allowed researchers to investigate complex unsteady and nonlinear flow phenomena, involving large unsteady flow structures. Today, both LDV and PIV are finding increasing use in ship propulsion studies.

The first LDV measurements about a marine propeller were made by Min (1978) in the variable pressure water tunnel at the Massachusetts Institute of Technology (MIT). These single-component measurements are considered landmark in providing the first time-varying velocity measurements about an operating propeller. This work was continued and extended by Kobayashi (1981), Kerwin (1982) and Yang *et al.* (1988) with measurements of time-averaged and blade-to-blade dependent flow though phase-averaging techniques. The combined use of LDV and phase-sampling techniques has allowed an efficient and robust reconstruction of the flow field along cross sections of the propeller wake and made possible the analysis of the turbulent flow about a propeller, which would otherwise be much more laborious and time consuming with conventional time-averaging techniques.

Following this approach, Jessup *et al.* (1985) conducted phase-locked LDV measurements about a marine propeller at very high angular resolution and showed the capability of the technique to probe the blade boundary layer as well as the flow around and between the blades. This experiment stimulated further measurements of the mean and fluctuating velocity distribution around a rotating propeller by LDV. Representative examples of these investigations are reported in Cenedese *et al.* (1985), Kakagawa and Takei (1986), Hoshino and Oshima (1987), Blaurock and Lammers (1988), Hoshino (1989, 1990).

Further insights into the complex laminar/turbulent flow about a typical research propeller were provided by Jessup (1989) with detailed three-dimensional LDV measurements upstream, downstream and through the propeller disk to define the general global flow, detailed blade boundary layer and blade wake characteristics in the near field of a marine propeller. The measurements by Jessup (1989) were adopted by the Propulsor Committees of the 20th and 21st ITTC as reference in a comparative experiment to map the near-field flow around the DTMB 4119 propeller by LDV.

The need for improved prediction of blade tip loading and tip vortex cavitation has focused significant interest on the detailed flow field associated with the tip vortex, specifically quantities such as the vortex core size, the velocity and vorticity distributions, and the morphology and physics of the roll up process. The primary difficulty with tip vortex measurement is the necessity to measure all three velocity components within a relatively small measurement volume (Kobayashi and Bugenhagen, 1985; and Jessup, 1989). Oshima (1994) measured a detailed map of the tip vortex flow by LDV for the purpose of validating a tip vortex inception prediction method. Chesnakas and Jessup (1998) provided a complete and detailed LDV investigation of the propeller tip vortex flow. The test matrix concerned a number of transversal planes downstream of the propeller

at four advance coefficients. The velocity samples were grouped into 1024 circumferential positions. The LDV set up was designed for coincident measurements of the three velocity components. For this purpose, two fiber-optic probes mounted on a two axis traverse system and arranged with the optical axis orthogonal to each other were used to measure the axial-tangential and the radial components of the velocity simultaneously. Results showed the structure of the vortex and provided details on the roll up mechanism of the blade trailing wake. Information was also obtained about the general wake structure and Reynolds stress quantities.

Stella *et al*. (2000) presented LDV measurements on tip vortex evolution within the near wake of the INSEAN E779 propeller model. Two different phase-sampling techniques, namely Angular Triggering Technique (ATT) and Tracking Triggering Technique (TTT), were presented and compared. Specifically, the tracking triggering technique, despite being less accurate, proved to be much more robust and efficient, and thus was recommended for test campaigns in which a large number of measurement points are to be interrogated. This study highlighted the obvious need for whole-field measurement techniques such as PIV for the propeller wake survey in the transition and far wakes.

While the aforementioned LDV studies on propellers operating in open water has comprehensively investigated the steady three-dimensional propeller wake in a blade-fixed reference frame, experimental surveys of actual propeller installation, on the other hand, are far fewer in comparison. In such cases, the experimental investigation of the propeller wake evolution in a given measurement plane requires a complete and adequately dense grid to be swept and eventually the adoption of phase-sampling techniques to resolve the wake evolution, a much more laborious and time consuming process. Rood and Anthony (1989) studied the flow interactions for a combined propeller–hull–appendage on an axisymmetric body along a transversal plane in front to the propeller disk and inside a sector of a circle of 90° in the upper left quadrant of the annular flow. Felli and Di Felice (2005) measured the phase-locked wake evolution around an installed propeller, using LDV and phase-sampling techniques. Measurements were made in the Large Cavitation Channel at INSEAN using the starboard half of a 6.4-m long twin-screw ship model. Both the propeller inflow and the downstream wake were measured by a two-component LDV system, sweeping twice Cartesian grids of about 400 positions each for the three-dimensional wake flow evolution. The lack of optical access in the region in front of the propeller limited the measurement to only the axial velocity component, whereas the survey of the complete three-dimensional wake was made downstream of the propeller.

LDV phase-sampling techniques were also used in the towing tank at INSEAN by Felli and Di Felice (2004) for the measurement of the three-dimensional wake flow along transversal sections of a twin screw ship model. More specifically, the authors focused on the dynamics of the tip vortex after the interaction with the rudder and provided an estimation of the hydrodynamic load distribution along the rudder span. Lubke and Mach (2004) used phase-locked LDV to measure the three-dimensional wake flow downstream of the propeller on a container ship. Measurements were carried out along a polar grid with 6 radial by 15 azimuthal positions.

Some applications of LDV are documented on rudder flow survey. Shen *et al*. (1997) carried out two-component LDV measurements in the Large Cavitation Channel at NSWCCD, on an 11.1 m surface ship model to measure the velocity field behind the propeller in the presence of the rudder. A more in-depth study on propeller-rudder interaction is documented by Felli *et al*. (2006, 2009), in which the wake flow evolution of a free running propeller-rudder configuration was investigated by phase-locked LDV. The investigations

concerned two transversal sections of the wake located just ahead and behind the rudder, each sampled through a grid of 800 points. In addition volumetric phase-locked LDV measurements were undertaken in the region where tip vortex reconnects after passing the rudder trailing edge, using a 20 x 20 x 20 point grid. Figure 1 documents the phase-locked distribution of the vorticity magnitude behind the trailing edge of the rudder and, specifically, the signature of the tip vortex re-connecting filament embedded in the trailing vorticity of the rudder. Recently, Muscari *et al*. (2010) studied the phase-locked wake evolution around an installed propeller-rudder configuration. Measurements were carried out in the stern region of a dummy model represented by the port-side of a twin screw vessel moving in straight course, along the vertical mid-plane of the rudder and three cross sections of the wake located in front and behind the rudder and at 75% chord (Figure 2).

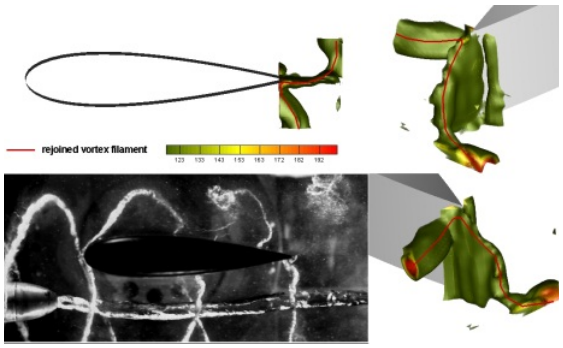

Figure 1 Volumetric LDV measurements about the tip vortex rejoining downstream of a rudder (Felli *et al*., 2009)

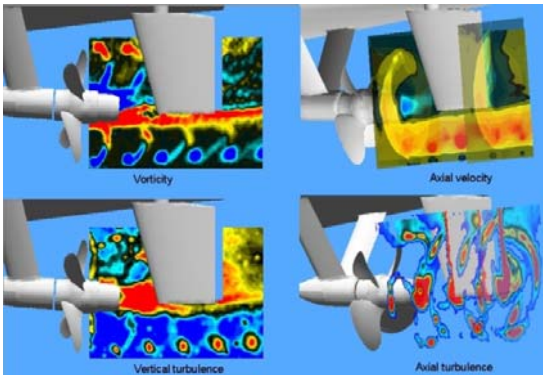

Figure 2 Wake evolution by phase-locked LDV measurements (Muscari *et al*., 2010)

LDV measurements are also documented for the survey of waterjets. In the cavitation tunnel at NSWCCD, Michael and Chesnakas (2004) measured the three dimensional flow of a waterjet pump (Figure 3). Velocity and pressure measurements were made at the inlet section, between the rotor and stator, at the nozzle exit and just downstream of the rotor. Archival-quality LDV flow measurements were presented also by Jessup *et al*. (2008). Atlar *et al*. (2007) used LDV to measure propeller race at various stations downstream of a podded propulsor in a cavitation tunnel.

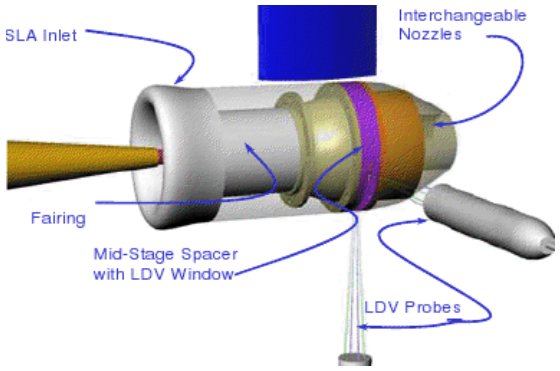

Figure 3 Three-dimensional LDV measurement set up for waterjet flow survey (Micheal and Chesnakas, 2004)

Since the late 90's, the need to explore more complex unsteady phenomena related to propeller flow highlighted the limitations of single-point techniques to capture the dynamics of unsteady large-scale eddies. Another major limitation for single-point measurements is the cost associated with extended facility operation required to achieve a whole velocity field with adequate spatial resolution, an issue especially severe in towing tanks. The development of PIV has partially overcome these limitations, expanding the range of applications to even more complex and critical problems.

The first successful application of PIV to the propeller wake flow analysis in non-cavitating condition is documented by Cotroni *et al*. (2000). The study used a replica of the set up in Stella *et al*. (2000) but analyzed the phase-locked wake evolution of the INSEAN E779 propeller along a longitudinal-radial plane. The survey of the propeller wake flow

from this new perspective highlighted the inadequacy of LDV, in which case a grid of large number of points would have to be swept to resolve adequately the dynamics of the wake structures. The authors introduced an iterative multi-grid approach and implemented window deformation to improve the quality of the raw-image processing, which is particularly critical in the analysis of flow in the presence of strong velocity gradients and coherent vortical structures. Today, these processing approaches are standard in general PIV analysis. Phase-locked measurements in a longitudinal-radial plane of a free running propeller wake were also made by Lee *et al*. (2002) by applying an adaptive hybrid two-frame particle tracking velocimetry (PTV) technique.

Di Felice *et al*. (2004) demonstrated the capability for PIV to identify the dynamics of dominant flow structures in the near wake of a propeller operating at different loading conditions. The authors pointed out that the effect of centrifugal force inside the tip vortex would spread out the seeding particles, and the obtained data would be locally biased because particles are acquired only when the vorticity is less than a given threshold. Paik *et al*. (2007) performed a similar study but focused on the analysis of the tip vortex geometry from the trailing edge down to one propeller diameter. Recently, Di Felice *et al*. (2011) presented a SPIV study on the evolution of the tip and hub vortices in the near wake of an open propeller.

Felli *et al*. (2006) used PIV and a rake of hydrophones to measure the phase-locked correlations between velocity and in-flow pressure fluctuations downstream of a marine propeller operating different advance ratios. The authors elucidated the onset of tip vortex instability in the interaction between the tip vortex and the trailing wake of consecutive spirals and highlighted a mechanism of energy transfer from the blade to the shaft harmonics in the transition wake. These aspects were studied in-depth by Felli *et al*. (2008) and Liefvendal *et al*. (2010) using LDV.

In the circulating water channel at MOERI, Paik *et al*. (2005) studied the effect of the free surface on the propeller wake of a container ship model. Phase-locked PIV measurements were performed on a vertical-longitudinal plane crossing the propeller axis at four different angular positions. The authors reported that the presence of the free surface affects the slope of the slipstream and the behavior of tip vortices.

A number of studies at NSWCCD applied PIV in the wake flow analysis of ducted propulsors and propellers in off-design conditions. Jiang *et al*. (1996) implemented Particle Displacement Velocimetry (PDV) to survey the vorticity and velocity distributions in the vicinity of a crashback propeller. Jessup *et al*. (2004) conducted PIV and LDV tests to investigate the unsteady separated flow around a conventional open propeller in extreme off-design conditions, including near bollard and crashback. This study was extended to the case of a ducted propeller in crashback operation by Jessup *et al*. (2006) which used SPIV to measure the unsteady flow (Figures 4 and 5). Chesnakas and Jessup (2003) conducted LDV and PIV experiments to measure in details the tip gap flow in a ducted propulsor. In this experiment the evolution of the leakage vortex in the gap of the blade tip and the duct inner surface and its unsteady interaction with the blade tip vortex was accurately measured.

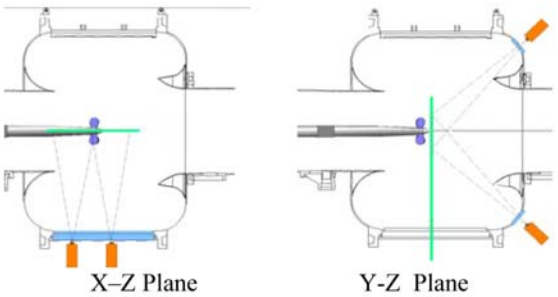

Figure 4 PIV and SPIV setup in Jessup *et al*. (2006)

Examples of PIV applications are also documented in the study of the wake flow around a propeller-rudder configuration. Felli *et al*. (2010) extended the work by Felli *et al*. (2006, 2009) by performing a comprehensive

study using PIV, LDV, and rudder-surface-pressure measurements to investigate the wake flow around a propeller-rudder configuration in free-running condition and behind a wake generator. The test matrix included PIV measurements at 3 horizontal-chordwise and 14 vertical-chordwise sections of the wake, LDV measurements at different transversal sections of the wake, each with a grid of about 700 points, and along the rudder surface with a grid of 1200 points. A sketch of the PIV planes and the LDV measurement grid is reported in Figure 6. The phase locked distribution of the out-of-plane vorticity is shown in Figure 7.

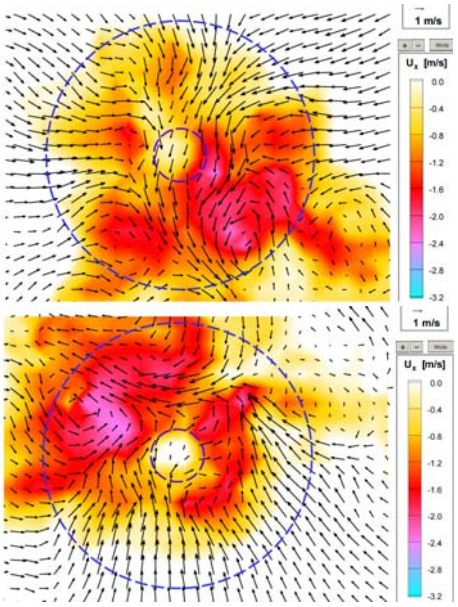

Figure 5 Propeller in crashback: instantaneous 3D velocity field at 0 and 3.1 seconds (Jessup *et al*., 2006)

Calcagno *et al*. (2002) applied stereo-PIV to measure the ship model wake flow in several cross-planes downstream of a 5 bladed propeller. The setup consisted of an underwater camera located 2 m downstream of the ship model and a dry camera imaging the measurement plane through the tunnel access window (Figure 8). The study illustrated the potential for SPIV for ship model wake flow testing and addressed critical issues in terms of data storage, management, and processing.

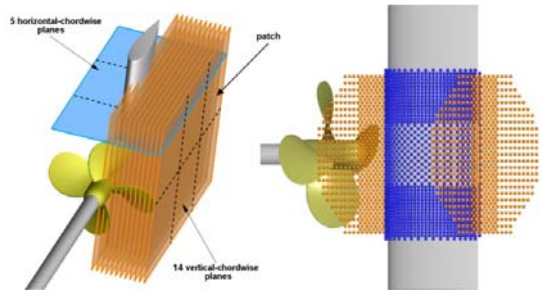

Figure 6 Measure of the propeller-rudder wake flow: PIV planes (left) and LDV grids (right) (Felli *et al*., 2010)

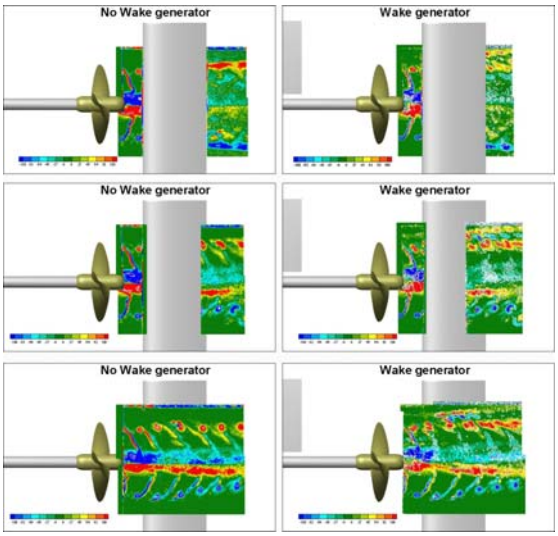

Figure 7 Distribution of the out of plane vorticity in some vertical-chordwise planes of the rudder flow (Felli *et al*., 2010)

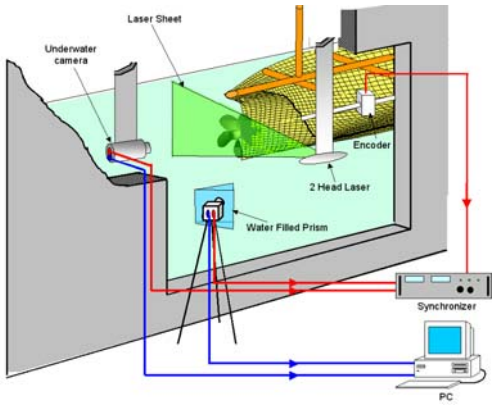

Figure 8 SPIV set up used in Calcagno *et al*. (2002)

Two-dimensional and stereo PIV were used by Wu *et al*. (2009) and Miorini *et al*. (2010) to study the morphology of flow structures in the rotor passage tip region of an axial waterjet pump. Measurements were performed in an

optically index-matched facility that enables unobstructed access to the entire flow field from any desired orientation. PIV data were acquired in meridional planes to investigate the evolution of tip leakage vortices. A sketch of the complex set up is documented in Figure 9.

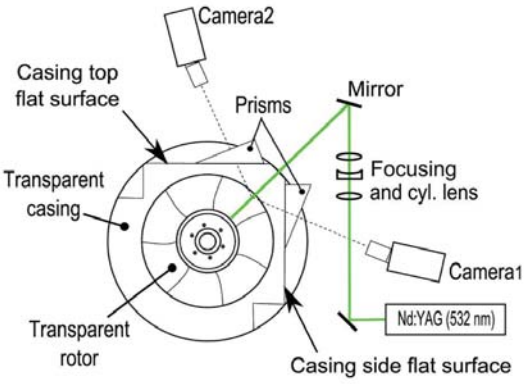

Figure 9 SPIV optical setup with cameras focusing on the tip region of the rotor blade in a waterjet (Miorini *et al*., 2010)

INSEAN developed the first underwater stereo-PIV system for towing tank applications. The system consists of a streamlined torpedo housing high-resolution cameras and laser optics that allow the measurement of all three components of velocity in a plane. The system is designed to be reconfigurable in several ways depending on testing needs. More details can be found in Felli *et al*. (2003). The system was used by El Lababidi *et al*. (2004) in the large cavitation channel at INSEAN to survey the evolution of the far wake of a dynamic positioning thruster. Other applications of the INSEAN system are described in Di Felice and Pereira (2007).

Following INSEAN, the use of SPIV underwater probes for towing tank applications has been rapidly spreading in many ITTC organizations. Anschau and Mach (2009) presented an SPIV investigation of the flow around a semi-balanced rudder on a surface vessel in steady drift. Specifically, the test matrix concerned two drift angles of the ship model, each with 5 rudder deflections. Measurements were conditioned upon the blade passage at 10 even-spaced angular positions of a six-bladed propeller and were taken in 29 planes aligned perpendicular to the moving direction of the towing carriage, 10 mm spaced to each other. At each plane, the phase-locked processing was performed on a population of only 10 records, which significantly degraded the quality of the statistical data. As this study is also related to ship maneuvering, it will be discussed in more details in Section 4.2 in the context of practical issues with the applications of this type of measurements in large-scale tow-tank facilities.

Other examples of SPIV applications in towing tanks are reported in Halmann *et al*. (2009), Bugalski (2009) and Nagaya *et al*. (2011) (Figure 10).

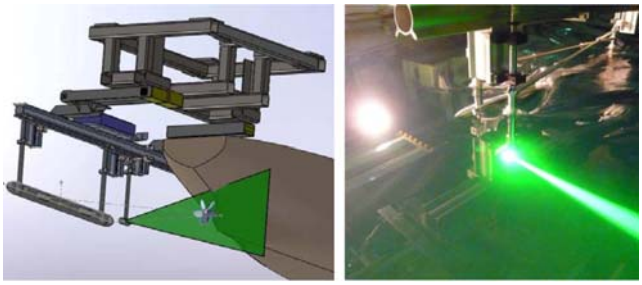

Figure 10 SPIV probe used in Nagaya *et al*. (2011)

Few examples of the application of detailed flow measurements to investigate propulsor hydrodynamics on full-scale vessels exist. Bull, *et al*. (2002) describe a collaborative effort by a consortium of research organizations, involving the measurements of the nominal and near-wake flow for two surface vessels at model scale. LDV was also utilized to measure a section of the inflow into the propeller in a full-scale trial. Starke *et al*. (2006) describe the European Full-Scale Flow Research and Technology (EFFORT) project, in which full-scale inflow velocity into the propellers were measured with LDV for several ships: two container ships, a tanker, a training vessel, and a hopper dredger.

Numerous examples of LDV and PIV measurements on hydrofoils as simplified geometry of propeller flows exist. Lurie (1993) performed a two-component LDV

measurement on a large foil (chord = 0.46 m) in the MIT cavitation tunnel to obtain steady and unsteady lift and drag performance. Billet (1987), Arndt and Dugué (1992), Fruman *et al*. (1992, 1993), Yamaguchi *et al*. (1995), and Pauchet (1996) measured tip vortices on elliptical and swept 3-D foils to study cavitation. Dong *et al*. (1997) utilizes a two-component LDV system to quantify vorticity, viscous and Reynolds stress in a technique to derive field and surface pressure on a hydrofoil at an 8-degree angle of attack. Bourgoyne *et al*. (2000, 2002) performed LDV and PIV measurements around the trailing edge and in the near wake of a very large hydrofoil at the Large Cavitation Channel at NSWCCD.

4.2 Applications of Detailed Flow Measurements in Ship Maneuvering

The applications of detailed flow measurements in ship maneuvering research have been extensively reviewed by the ITTC Manoeuvring Committee at the 21st, 22nd, 23rd, 24th and 25th ITTC conferences. This review summarizes those findings, adds new perspectives regarding practical issues on the application of detailed flow measurements, and supplements with new developments since the 25th conference.

While the applications of flow measurement techniques in the ship propulsion community date back to the late ’70s, such practice did not find notable adoption in the ship maneuvering field until the mid ’90s. In the 1980s and early 1990s, various semi-empirical modelling techniques were attempted in order to capture nonlinear and viscous aspects of maneuvering problems. Hirano and Takashina (1980) proposed a hull force model based on captive model test results that took into account nonlinear coupling between yaw and roll. Kose *et al*. (1992) developed a database approach for the prediction of hydrodynamic forces and moments around the hull and discussed the need for specific database for each ship type. Kajima and Tanaka (1992) and Tanaka and Kajima (1993) proposed a prediction method that included a cross-flow drag contribution to the hull, with generally good comparison to experimental data.

While these modelling techniques may represent very practical approaches to the prediction of ship maneuvering characteristics, they share a similarity in the fact that they attempt to capture complex viscous flow phenomena by trying to model the “effects” rather than the “physics” of the problem. Thus they rely heavily on the availability of experimental data, which often times need to be specific to the hull form and must cover the range of operating conditions that the ship is expected to encounter during its lifetime. Advanced experimentation included the usage of segmented models to measure the distribution of forces along the hull (Hooft 1994), and little emphasis was placed on comparison of numerical results with measurements of complex viscous flow fields.

Another important practical factor which contributed to the relatively late adoption of detailed flow measurements to the ship maneuvering field is the fact that experimental investigations of ship maneuvering almost always occur in a basin. Many challenges exist with the application of LDV or PIV in large-scale tow tank facilities, specifically the low level of testing economy and the high complexity of test setup. While LDV was finding wide usage in cavitation tunnels in the measurement of propeller flows in the ’80s and ’90s, similar measurements in a test basin to map out large sections around a hull to observe patterns of cross flow separation for a maneuvering ship or submarine would have been comparatively prohibitive in cost.

Since the ’90s, there has been significant advancement in physics-based tools such as RANS and potential flow codes coupled with various models to account for complex viscous phenomena such as the vortex lattice technique. With the increasing applications of these tools on ship maneuvering problems, the need for detailed flow information for validation

purposes became more and more critical. While traditional methods of analysis such as coefficient-based simulation or system identification are concerned primarily with the hydrodynamic coefficients associated with a hull form or the trajectory of a free running model during a maneuver, the accuracy of a viscous flow code in the prediction of ship maneuvers would be highly dependent upon its ability to predict physical phenomena such as cross-flow separation or the interaction of large-scale vortical structures with the afterbody.

Hearn and Clark (1993) extended slender body theory to include the effects of stern vortices on the development of forces and moments on the hull. Ohmori and Miyata (1993) and Ohmori *et al*. (1994) applied RANS to calculate the flow around a ship hull in oblique tow. These developments provided the impetus to perform more complex experiments to investigate the flow fields around maneuvering ships. Nonaka *et al*. (1995) performed an experimental investigation on three VLCC ship models with different shaped sterns in oblique towing motions. Measurements included the overall forces and moments on the hull, flow field in the stern region using 5-hole pitot probes, and visualization of separation regions by tufts. Relationship among stern shape, flow field, and hydrodynamic forces were discussed. Ando *et al*. (1997) and Nakatake *et al*. (1998) developed a surface panel method and presented results comparing numerical solutions with the experimental results by Nonaka *et al*. (1995). Kijima *et al*. (1995, 1996) also used the same experimental results in comparison to their estimation method of hull forces and moments using a cross flow drag term based on a vortex shedding model and separation line from captive model experiments.

Longo and Stern (1996) applied 5-hole pitot probes to measure the time mean velocities around a series 60 C_B=0.60 ship model at angles of drift, along several longitudinal stations. Wave profiles and local and global elevations using capacitance and servo probes were also measured to assess the nature of the interaction between ship-induced wavemaking with the boundary layer and wake. This extensive dataset were heavily used for the purposes of CFD validation by various researchers (Campana *et al*., 1998; Alessandrini and Delhommeau, 1998; Tahara, 1999; and Tahara *et al*., 2002). Di Felice and Mauro (1999) performed a series of experiments on the same hull form in a double-model configuration at a very large drift angle of 35 degrees and measured the mean cross-flow velocities using LDV.

Two-component PIV was used to interrogate flow in the near wake of the ESSO Osaka model at static hull drift and rudder angles (Simonsen and Stern, 2005). Several X-Y planes parallel to the water surface and X-Z planes parallel to the center plane of the ship were interrogated. The authors reported that the PIV data were "not as good as hoped for," possibly due to the fact that 2D PIV was used to measured a strongly three-dimensional flow.

As previously described, Anschau and Mach (2009) presented an SPIV investigation of the flow around a semi-balanced rudder on a surface vessel in steady drift, a situation very similar to the study by Simonsen and Stern (2005). While the use of stereoscopic PIV may have alleviated the bias due to out-of-plane velocities as observed in Simonsen and Stern, this study highlights other practical issues associated with the performance of this type of measurements in non straight-flight conditions. The PIV system utilized in that study was set up to measure flow in a plane perpendicular to the carriage travel direction. The plane of measurement, therefore, achieved a transverse cut in the ship-fixed frame only for the case of zero model angle of drift; while preferably for CFD validation purposes, the transverse cut should always be in the ship-fixed reference frame. Also as previously mentioned, only 10 PIV records were collected for each propeller angular position, which significantly degraded the quality of the statistical data. The primary

reason for the low quantity of data is the limited number of runs per hour associated with testing in a towing basin.

Another example of SPIV measurement around the propeller and rudder of a surface vessel in a maneuvering condition was performed by Atsavapranee *et al*. (2010) with the DTMB model 5617 (a geosym of DTMB model 5415) in the Rotating Arm Basin at the NSWCCD. The primary focus of the study was to investigate the effect of cross flow on the side force generated on the propellers and the lift generated on the rudders when the ship is in a steady turn. SPIV measurements were performed to measure the nominal wake at the propeller reference plane, the inflow into the rudders, and in the near wake at several downstream stations. Thrust, torque, and side forces on the propellers and lift generated on the rudders were measured and correlated with the flow field.

In the study by Atsavapranee *et al*. (2010), a special mounting frame holding the SPIV cameras and laser optics housings was constructed and mounted to the same carriage sub-structure supporting the ship model. This setup allowed the entire SPIV setup to rotate with the hull as the ship model was set at different angles of drift and turning radii. In such a way, the interrogation plane was always in the transversal plane relative to the body-fixed coordinate system (except for a small dynamic trim the model achieved at speed). Furthermore, the mounting frame holding the cameras and lasers could be traversed in the longitudinal direction, allowing different transversal planes to be interrogated without reconfiguring the hardware or repeating the SPIV calibration process. Although this setup overcame some of the limitations of the setup by Anschau and Mach (2009), it was at a cost of significant added complexity. A CAD rendering of the setup is illustrated in Figure 11.

As was the case of Anschau and Mach (2009), Atsavapranee *et al*. (2010) also suffered from the poor economy (PIV records per hour) associated with measurements in a basin. Due to this fact, time-averaged rather than phase-locked measurements were performed to achieve good statistical data within a reasonable number of testing days. Since the primary quantities of interest were the average thrust, torque and side forces on the propellers and lift on the rudders, time-averaged flow field was deemed adequate. An example of these time-averaged SPIV measurements is shown in Figure 12.

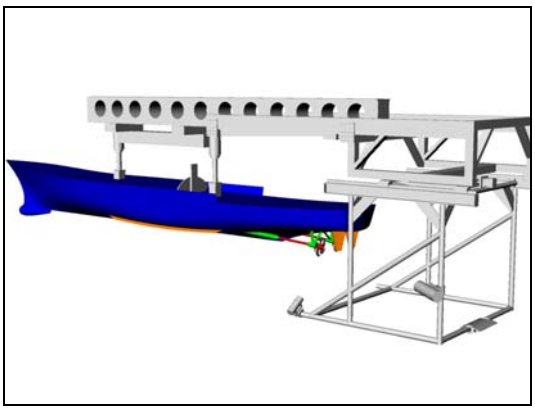

Figure 11 SPIV setup used in Atsavapranee *et al*. (2010)

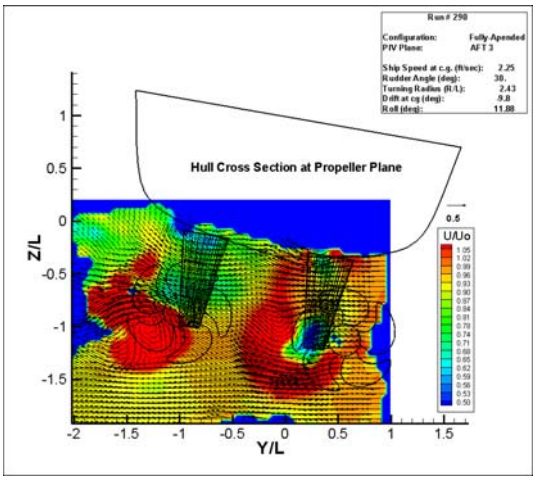

Figure 12 Example of time-averaged SPIV measurement in the near wake of a surface vessel in a steady turn, from Atsavapranee *et al*. (2010)

Also starting in the mid 90's, many experimental activities involving detailed flow measurements on submerged vessels has been documented. In 1994, Liu *et al*. reported a demonstration of the use of PIV to measure

flow structures around a submarine model in the Rotating Arm Basin at NSWCCD. The study both represents an important milestone and highlights many technical challenges associated with the application of flow measurement techniques in large-scale tow-tank facilities (setup complexity, available laser power, camera sensitivity, etc). Fu *et al*. (2002) performed a similar experiment with a much more advanced system, measuring the flow in a cross-plane around the submarine model, ONR Body-1, in rotation using a submersible PIV system fixed to the basin. In that study, a 120 mJ/pulse flashlamp-pumped dye laser coupled to an optical fiber was used to deliver the laser light which was formed into a laser sheet by a series of optical lenses in a submersible housing. Atsavapranee *et al*. (2004) performed SPIV, force and moment, and pressure distribution measurements around the same model towed in a straight course at angles of drift in the Shallow Water Basin at NSWCCD using a more powerful dye laser (1 J/pulse) with high-resolution (2K x 2K) submersible cameras mounted on a hydraulic platform. The hydraulic platform was installed in the middle of the basin and raised above the water surface for the installation of the SPIV hardware in situ. The platform was lowered to submerge the cameras and the laser sheet for the calibration of the SPIV system. Finally, the system was lowered to test depth and the measurements performed as the model was towed through the light sheet, effectively interrogating successive cross planes along the hull and the downstream wake. A CAD rendering of the experimental setup is illustrated in Figure 13.

Using basin-fixed PIV systems (rather than a "towed" PIV system), studies by Liu *et al*. (1994), Fu *et al*. (2002) and Atsavapranee *et al*. (2004) were also limited by the fact that the planes of measurements were not aligned with the transversal plane in the ship-fixed coordinate system. In Atsavapranee *et al*. (2004), the case is similar to Anschau and Mach (2009) (section 4.1) in that the light sheet was set perpendicular to the tow direction and the measurement plane coincides with the transversal plane only at zero model angle of drift. In Liu *et al*. (1994) and Fu *et al*. (2002), the angle that the light sheet made to the model actually varied over the length of the model as the model was towed through the light sheet in rotation, as illustrated in Figure 14.

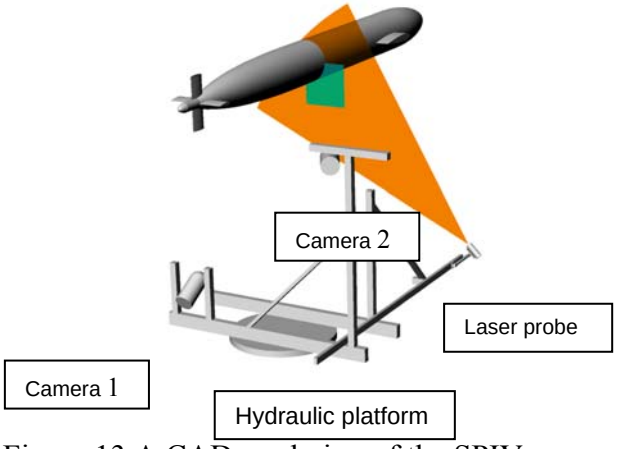

Figure 13 A CAD rendering of the SPIV measurement setup in a straight-line basin from Atsavapranee *et al*. (2004)

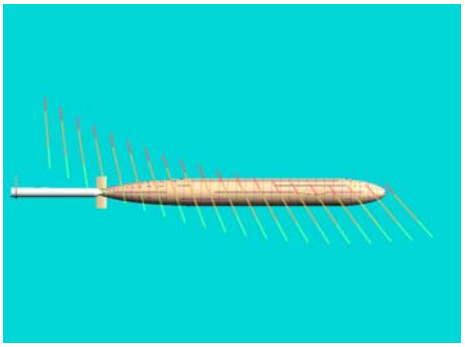

Figure 14 Locations of PIV measurement planes along the hull in a rotating arm basin experiment from Fu *et al*. (2002)

The first application of a towed PIV system for the study of maneuvering ship was reported by Longo *et al*. (2006) on a comprehensive set of PMM experiments performed with the DTMB 5512 model with PIV measurements conducted at the propeller plane. In this study, the PIV system was supported by the PMM carriage and followed the model during its oscillatory motion. The experiment was part of the Workshop on Verification and Validation of Ship Maneuvering Simulation Methods (SIMMAN 2008) held in Copenhagen,

Denmark in April 2008. The workshop represented the first organized international effort to benchmark maneuvering predictive capabilities through systematic quantitative validation with high-quality experimental data. Simulation results were compared with extensive experimental data sets for tanker, container ship and surface combatant hull form test cases. The results of the workshop were described in details in the 25th Maneuvering Committee final report.

Etabari *et al*. (2008) utilized the same basic hardware as used in Atsavapranee *et al*. (2004) to investigate the hydrodynamics around a submarine model, SUBOFF, in a steady rotation experiment at NSWCCD. In this case, the SPIV hardware was fixed to rotate with the model for an arbitrary angle of drift and turning radius. Flow field and pressure distribution were measured at two discrete transversal planes, in addition to the measurements of total forces and moments on the hull. Figures 15 and 16 illustrate the SPIV setup used to interrogate the forward and aft transverse stations. Figure 17 presents an example of the measurement results at $x/L = 0.84$.

It is apparent that the conduction of PIV or SPIV measurement in which the PIV system is towed, especially for a submerged model, can involve a very complex setup. Practical issues regarding the delivery of laser power, the design and the interference effects of the support structure, and the customization of new hardware to existing facility remain important challenges. In order to reconfigure the system from measurement in the forward plane to the aft plane in Etebari *et al*. (2008), the structure had to be physically removed and reassembled, requiring recalibration of the SPIV setup and significant drydock time. Recent development at NSWCCD has made possible SPIV measurement at multiple transversal planes along a submerged vessel using a traversable frame structure similar to that used for a surface vessel in Atsavapranee *et al*. (2010).

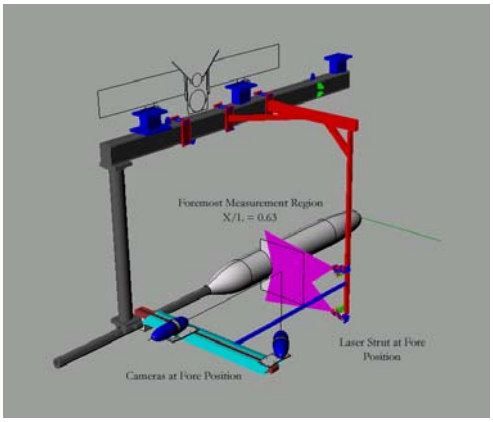

Figure 15 SPIV setup for the measurement along the parallel midbody of the SUBOFF model from Etebari *et al*. (2008)

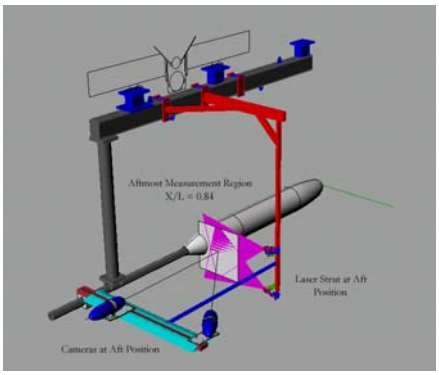

Figure 16 SPIV setup for the measurement along the aftbody of the SUBOFF model from Etebari *et al*. (2008)

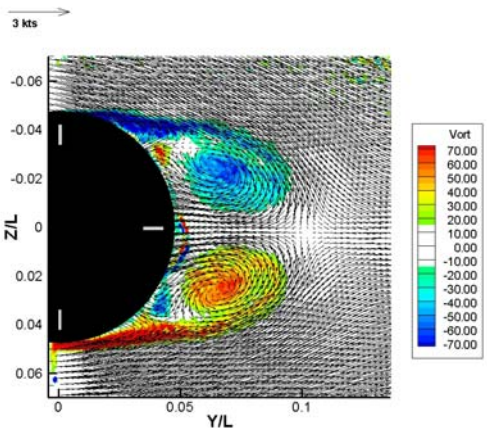

Figure 17 Example of SPIV measurement along the aft body of the SUBOFF model in rotation

4.3 Applications of Detailed Flow Measurements in Ship Seakeeping and Free-Surface Flows

Potential-flow strip theories or 3-D panel methods represent a class of very efficient and accurate numerical tools for the prediction of seakeeping problems such as wave loads and wave-induced ship motions, especially in the linear regime. Even for some nonlinear problems, such as vessels with flared bows and sterns or ships in nonlinear wave environments, advanced techniques such as time-domain nonlinear strip methods or panel methods can be applied. However, when nonlinear viscous phenomena such as wave breaking, bow slamming, green water, or roll damping are concerned, viscous flow computations are generally necessary to deal with these problems.

With the rapid development of CFD since the mid 90's, researchers are now utilizing tools such as U RANS to address the full 6DOF ship motions in wave environment. Coupled with this development has been the application of detailed flow measurements such as LDV and PIV and various wave-field measurement techniques to increase understanding of the flow phenomena and to obtain benchmark experimental data for the validation of CFD tools. Toda *et al*. (1992) applied 5-hole pitot probes to measure the time mean velocities around a series 60 ship model with C_B=0.60 at several longitudinal stations. Wave profiles using capacitance and servo probes were also measured to assess the nature of the interaction between ship-induced wavemaking with the boundary layer and wake. Longo and Stern (1996) performed similar measurements for the same model at different angles of drift. Longo *et al*. (1998) utilized LDV to quantify the mean flow and Reynolds stresses around a surface-piercing flat plate in a towing tank. The experiment, although canonical in nature, has wide implications to situations in which a solid/free-surface juncture boundary-layer flow exists, such as at the waterline of a ship.

In 1997, Dong *et al*. utilized PIV in the 140-ft basin at NSWCCD to characterize flow within the attached liquid sheet upstream of the bow wave separation point on a realistic 3m-long surface vessel model. Roth *et al*. (1998) performed a similar measurement but on a 7m-long model at a higher Reynolds number, allowing finer observation of the flow structure.

In addition to flow-field measurements, experimental measurements of free-surface elevations for steady and unsteady problems are also of great interest. Accurate prediction of wave elevation close to the hull is related to bow-wave breaking, wave load on blow flare and deck wetness, and far-field waves are correlated with the damping of ship motions and added resistance in waves. Ohkusu (1980) proposed a method for measuring waves generated by a ship moving at a constant forward speed by means of capacitance probes fixed in the towing tank performing measurements along longitudinal lines parallel to the ship advance direction. Transformation of the basin-fixed line measurements was performed to compute instantaneous wave field around the hull in the ship-fixed frame of reference, and the results were used to predict the added resistance. Ohkusu and Wen (1996) and Ohkusu and Yasunaga (2000) extended this technique to analyze cases with incident waves and sinusoidal ship motions. The measured wave field was decomposed into a steady component (Kelvin waves), a fundamental component (linear component due to body motion), and a second harmonics (nonlinear component due to second-order effects).

The combatant hull form as represented by DTMB model 5415 has been used widely in various hydrodynamic studies, primarily for the purpose of CFD validation, by many ITTC organizations throughout the years. Stern *et al*. (2000) described an international collaboration to develop benchmark CFD validation data on the 5415 hull form. Overlapping tow tank tests between three institutes (IIHR, INSEAN, and NSWCCD) measuring resistance, sinkage and trim, wave profile and elevation, and nominal

wake using pitot probes were performed using the same hull geometry at different scales (DTMB model 5512, DTMB model 5415, and INSEAN model 2340A). Apart from the overlapping tests, each institute also performed unique sets of experiments. Ratcliffe (2000) utilized the 5415 bare model fitted with shafts and struts, and performed experiments with and without propellers. Measurements include free surface topography around the transom using servo probes, wave field around the hull using longitudinal wave cuts, and flow field upstream and downstream of the operating propellers using LDV. Gui *et al*. (2000) employed wave probes attached to the moving carriage to obtain detailed information such as free-surface turbulence and high frequency responses for the DTMB model 5512 advancing in regular head waves, but restrained from motions. Coupled with the use of basin-fixed wave gages spaced every $\Delta y=0.1$, high-resolution and time-resolved wave field around the hull was obtained. At INSEAN, a comprehensive flow mapping of the boundary layer and wake flow was performed on the model 2340A at eleven cross planes with pitot probes.

Following this cooperative effort, the same consortium (IIHR , INSEAN, and NSWCCD) collaborated further on a complex viscous hydrodynamic problem of a surface vessel in roll. Roll motion on a surface vessel is lightly damped and lightly restored and is difficult to predict due to viscous phenomena such as vortex separation from the bilge keels. For this study, the three institutes focused on the same hull form (DTMB 5415) but with the addition of hull appendages including the bilge keels. Single-degree-of-freedom roll decay tests were performed at various forward speeds, with comprehensive measurements including two-component LDV measurements along eight transversal planes at INSEAN (Felli *et al*. 2004), wave-field and PIV measurement at IIHR (Irvine *et al*. 2004), and PIV and force and moment measurements at NSWCCD (Bishop *et al*., 2004). The PIV data was used to correlate with the bilge keel lateral force and validate CFD with encouraging results. Figure 18 and 19 illustrate the comparison of the roll time history and the flow around the bilge keel at a cross plane of the vessel between the experimental data by Bishop *et al*. (2004) and the URANS solutions by Miller *et al*. (2008).

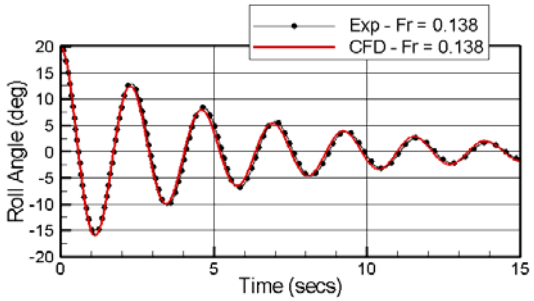

Figure 18 Comparison of the free roll-decay time history between experiment and CFD for the DTMB 5415 hull form at Fr = 0.138

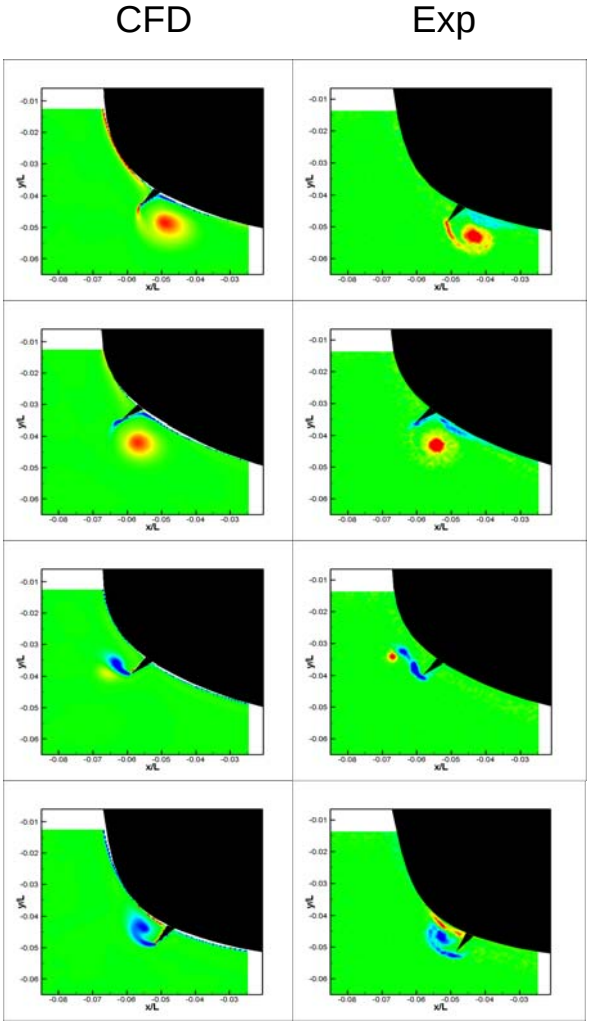

Figure 19 Comparison between CFD and experiment of the flow around the bilge keel of the DTMB 5415 at the LCG plane at Fr = 0.138

During a follow-on phase of this collaborative effort, a calm-water roll-decay trial was performed on the Italian vessel, *Nave Bettica*, (Atsavapranee *et al*., 2008). Viscous flow field around the port bilge keel of the *Bettica* was measured using PIV, along with the lateral force on the bilge keel using surface-mounted strain gages. This study represents the first application of the PIV technique on a full-scale vessel. The installation of the PIV system was planned to coincide with a normal drydock period for the ship, and thus did not impact the ship operational schedule. Figure 20 illustrates the complex setup of the PIV system. Figure 21 shows an example of the PIV measurement obtained during the trial.

Figure 20 PIV setup on the Italian vessel, *Nave Bettica*, from Atsavapranee *et al*. (2008)

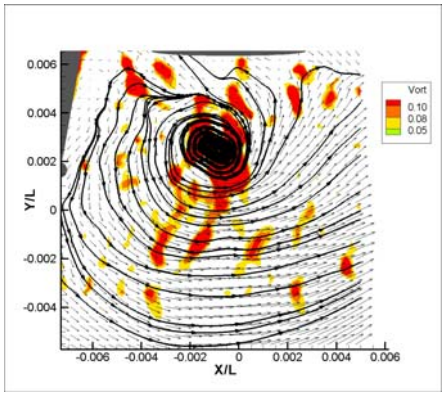

Figure 21 Example of PIV measurement around the port bilge keel of the Italian vessel, *Nave Bettica*, performing a calm-water roll-decay at 12.8-knot (Atsavapranee *et al*., 2008)

A number of investigations have recently focused on the breaking waves around a surface vessel as these are the main source of air entrainment and "white water" in the vessel wake. Waniewski *et al*. (2002) experimentally characterized a simulated bow wave produced using a stationary deflecting plate in recirculating water channel and additionally a wedge model in a tow tank. Both contact line measurement using capacitance probes and wave profile measurements using a resistive wave gage were performed. Attempts were also made to characterize the shape of the plunging jet, with a limited success due to the intrusive nature of the wave gage. Broglia *et al*. (2004) performed a RANS computation of the problem using the single-phase level set approach for interface capturing and found good general agreement with the experimental data. Karion *et al*. (2003) used a laser-sheet technique called *QVIS* to profile the breaking bow waves on large 20-degree and 40-degree wedge models. Fu *et al.* (2005) and Fu *et al.* (2006) conducted detailed measurements to characterize the wave field around the DTMB model 5365, which is a model of the *R/V Athena I*, and also on the full-scale ship itself.

5. CURRENT AND EMERGING DETAILED FLOW MEASUREMENT TECHNIQUES

5.1 Flow-field Measurements

5.1.1 Conventional Flow-Field Measurement Techniques

In recent years, laser-based flow measurement techniques have become increasingly popular and are now used in applications in which intrusive techniques proved to be inadequate. Typical examples range from ship wakes to propeller flows and hydrodynamics of underwater vehicles. To date, Laser Doppler Velocimetry (LDV) and Particle Image Velocimetry (PIV) represent the most widely used detailed flow measurement techniques in naval hydrodynamics.

Laser Doppler Velocimetry (LDV) is a well-established technique for detailed flow measurements in the hydrodynamic field and is routinely used in many naval research organizations throughout the world. The working principle is based on the use of the coherent wave nature of laser light. The crossing of two laser beams of the same wavelength produces areas of constructive and destructive interference patterns. This "fringe" pattern is composed of planar layers of high and low intensity light. Velocity measurements are made when seeding particles in the flow pass through the fringe pattern, scattering the laser light, which is collected by a detector and analyzed by a signal processor to measure the corresponding Doppler frequency. The Doppler frequency is proportional to a component of particle velocity normal to the planar fringe pattern. An exhaustive description of the technique can be found in Drain (1980).

The particular advantage of the LDV technique is the ability to accurately measure all three velocity components even in highly turbulent flows and in flows with recirculation zones, at high temporal and spatial resolution. These characteristics have made LDV suitable for the survey of complex three-dimensional flow around propellers, appendages and ship wakes (e.g., Chesnakas and Jessup, 1998; Felli and Di Felice, 2005; Jessup *et al*., 2008; and Felli *et al*., 2009). On the other hand, LDV is fundamentally a point measurement technique: the time evolution of velocity can be measured with great accuracy at a point, but if a map of an area of the flow is to be obtained, it must be built up point by point. This characteristic makes LDV most suitable for flows that are either steady or highly repeatable and highlights the limitation of the technique in the spatial characterization of unsteady large-scale coherent structures. From the logistical point of view, extended periods of facility operation are typically required if a large area has to be investigated at an adequate spatial resolution. This aspect becomes particularly critical to applications in tow tanks, where the limited length can heavily impact the productivity of the measurement and consequently on the operational cost of the test.

The relatively recent development of Particle Image Velocimetry (PIV) has overcome most of the limitations of LDV. In particular, the redued time required to obtain a statistical set of data has brought a significant savings in the testing costs. Also being an instantaneous planar measurement technique, PIV has made possible the characterization of unsteady large scale vortical structures.

The basic principle of PIV involves seeding the flow with tracer particles which are illuminated by a sheet of laser light. Two images of the region of interest are recorded at two successive instants in time by a high-resolution digital camera. The "flow record" of the whole 2D field is then divided into a grid of interrogation cells, and in each cell, the average distance that the tracer particles move from the first image to the second is determined using a cross-correlation technique. Knowing the distance travelled and the time taken, the velocity of the flow in that cell, therefore, can be calculated. This process is repeated for every cell, giving a 2D map of the "instantaneous" velocity field at the recording time. More details about the technique are reported in Raffel *et al*. (2007).

Stereoscopic PIV is an extension of planar-PIV to applications in which the presence of strong three-dimensional coherent structures and velocity gradients requires all velocity components to be measured. The technique is based on the principle of stereoscopic imaging. Two cameras are arranged to image the illuminated flow particles from different perspectives. The combination of both camera projections allows the reconstruction of the three-dimensional particle displacement inside the measurement volume and the evaluation of all three velocity components.

5.1.2 Emerging Flow-Field Measurement Techniques

Today's challenging problems in naval hydrodynamics concern complex three-dimensional unsteady flows for which standard and stereoscopic PIV approaches provide only a partial limited view of the global problem. Significant interest exists in the application of full three-dimensional flow-field measurement techniques to characterize the topology and the dynamics of unsteady flow structures in separated and reattached flows, flows in off-design conditions, and destabilized wake flows. This trend has motivated the development of frontier techniques whose validation and assessment on real cases has yet to be performed, at least in naval hydrodynamics. In this scenario, complexity of technologies and setups has to be considered and consequently new critical issues have to be addressed.

PIV, as a three-component (3C) and three-dimentional (3D) volumetric technique, is not yet well established, and various approaches are still being investigated. In the last fifteen years, some hybrid solutions, such as multi-plane (Kahler and Kompenhans, 2000) and multi-layer (Abe *et al*., 1998) PIV have been developed to measure the simultaneous three velocity components in more than one plane. However, these approaches suffer from extreme complexity, inadequate spatial or temporal resolution and/or lack of capability to measure both size (such as that of a bubble nucleus) and velocity data.

Fully 3C-3D measurement are currently only feasible though adjustable-depth volume PIV techniques, such as 3D-particle tracking velocimetry (Maas *et al*. 1993), holographic PIV (Pu and Meng, 2000; Hinsch, 2002), tomographic PIV (Elsinga *et al*., 2006) and defocusing PIV (Willert, 1992). These techniques use expanded beam illumination while still maintaining normal viewing. The illumination sets the depth of the recorded 3D region while the field area is limited by either the sensor size or the imaging ratio.

Three-dimensional Particle Tracking Velocimetry (3D-PTV) is a powerful measurement technique that allows Lagrangian flow information to be obtained directly from measured 3D trajectories of individual particles. The three velocity components are obtained by identifying and tracking the positions of the trace particles as they move through the observation volume. Particle density is a critical parameter in SPTV and dictates the spatial resolution of the measurement. Specifically, seed concentration must be adequate to allow a reliable identification of each single particle, at least in three of the four cameras. Moreover, the average displacements of traces must be small compared to the mean spacing among particles.

Holographic techniques such as HPIV are highly esteemed for their suitability for the studies of complicated three-dimensional fields and bubbly flows (e.g. Katz *et al*., 1983). However, the application of holography has not been widely embraced for non-laboratory experiments because of the inherent complexity and the sensitivity to external perturbations which are difficult to control in hydrodynamics facilities. In addition, the interrogation process of the holograms is a time-consuming operation and requires much computational efforts to extract displacement data.

Tomographic PIV is a recently developed technique that records the tracer particle images from several directions simultaneously and uses tomography to reconstruct the particle distribution within the illuminated volume as a 3D light intensity map. The velocity field is obtained from cross-correlation of two 3D intensity maps corresponding to subsequent exposures of the particle images. The working principle is, therefore, closely related to the long and successful development of 3D Particle Tracking Velocimetry with the added benefit being the fact that much higher seeding densities can be handled. Tomographic PIV is currently considered a very attractive technique even if the requirement of multi-angle viewing for the volumetric reconstruction of the three

velocity components restricts its application to laboratory-scale test cases.

Defocusing Digital Particle Image Velocimetry (DDPIV) technique is a new approach in mapping the three-dimensional flow field, based on the defocus principle to identify the three-dimensional particle locations within the illuminated volume. A volumetric cross correlation is computed to estimate the velocity field. Besides the applicability as a velocimetry technique, DDPIV is capable of real-time imaging of bubbly flows, providing size characteristics of the bubble phase, e.g. population density and void fraction, within a volume (Pereira and Gharib, 2004). DDPIV was applied to the two-phase flow-field around a propeller by Pereira *et al*. (2006) and Pereira (2011). Figures 22 and 23 illustrate examples of velocity and void fraction measurements from Pereira (2011).

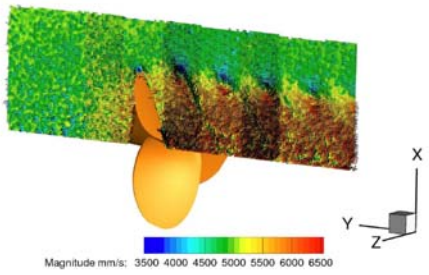

Figure 22 Sample velocity field measurement using the DDPIV technique (Pereira, 2011)

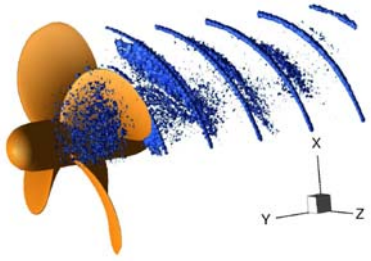

Figure 22 Sample void fraction measurement using the DDPIV technique (Pereira, 2011)

Particle Shadow Velocimetry (PSV, Goss *et al*., 2007a) is a novel technique, which shares many of the attributes of microPIV (Santiago *et al*. 1998) and Forward Scatter PIV (fsPIV, Ovryn *et al*., 2000). It utilizes low-power, pulsed light sources such as LEDs to measure the displacement of seed particles in a flow field, suitable both in liquid and gaseous flows. Being a volumetric illumination technique, it relies on the receiver optics to minimize the depth of measurement. Any pulsed light system can be used as the light source; however, LEDs are particularly well suited since they can be overdriven in a short-pulse mode to produce intense sub-microsecond light pulses. Because the technique does not rely upon weak particle light scattering, lasers are neither necessary nor recommended with this approach.

The use of LEDs as a light source provides several advantages. The first is the possibility of repetitive pulses in a single frame for particle tracking. The use of color eliminates the need for cross-correlation cameras and the laser, a significant reduction in equipment cost. Volumetric illumination eliminates the strong reflections on surfaces; thus measurements can be made as close as 10-micrometers to a surface. High pulse rates, on the order of kHz, can be achieved with LED illumination. Furthermore, the use of multi-color LEDs offers the potential for simultaneous velocity and acceleration measurements, (Goss *et al*., 2007b and McPhail *et al*., 2010).

Surface Stress Sensitive Film (S3F) provides a novel method for the measurement of the flow induced surface stress distribution on aero- and hydrodynamic surfaces (Crafton *et al*., 2008). The measurement of skin friction on hydrodynamic surfaces is of significant value for the design of advanced naval platforms, particularly at high Reynolds numbers. The S3F sensor was developed for measurement of skin friction and pressure on a surface that operates in both air and water. The sensor is based on an elastic polymer film that is applied to a surface and deforms under the action of applied normal and tangential loads by a fluid flowing over the surface. Skin friction and pressure gradients are determined

by monitoring these deformations and then solving an inverse problem using a finite element model of the elastic film. Crafton *et al.* (2008) describes the development of a sensor package specifically designed for two-dimensional skin friction measurements at a single point, but the method has been successfully transitioned into a 2D planar surface providing a unique capability for flow induced wall shear measurement. Quantitative measurements of skin friction have been performed in a high Reynolds number turbulent boundary layer. The results indicate that the sensor skin friction measurements are accurate to better than 5%, repeatable to better than 2%, and show good quantitative definition of flow direction. The sensor is sensitive to pressure gradients, not to static pressure and should be useful for monitoring the skin friction on seafaring vessels operating over varying depths where static pressure variation will occur.

5.2 Wave-Field Measurements

5.2.1 Conventional Wave Measurement Techniques

5.2.1.1 Intrusive Wave Measurement Systems

A variety of wave measurement systems have been used in test tanks over the last fifty years. The majority of these systems have been intrusive, requiring a sensor to be placed in contact with the water. Common intrusive devices used are resistance, capacitance and servo-mechanical (finger) probes.

Resistance probes use two parallel wires, normally mounted vertically into the water. The electrical resistance between the wires is measured and the immersion of the probe inferred from this. These systems are reliable, easy to use, and moderately priced, and have been widely used for many years. Results depend on the water conductivity which can vary with temperature; probes require regular calibration. Capacitance wave probes measure the capacitance between a wire and the water. The wire is insulated from the water with a thin uniform waterproof dielectric coating.

Servo-controlled wave probes use a metal needle moving vertically and controlled by a closed-loop actuation system, so that the needle closely tracks the water surface. The conductance between the head of the needle and the water is measured to detect the change in medium (air or water), and the needle position moved rapidly in and out of the water. Servo-controlled probes are limited in both range and vertical velocity and are sensitive to dust particles on the water surface.

Well-known difficulties with intrusive probes include effects due to meniscus reversal and scattering of waves around the wires. In large waves (e.g. more than 0.5 m), when long probes are required, fluid loading on the probes can cause vibration affecting separation of the wires and hence resistance or capacitance. Problems are exacerbated in the presence of non-zero mean flow speed, when ventilation can occur, as air is sucked down the low-pressure side of the wires; run-up may also occur on the high-pressure side of the wire. Challenges can also be faced in very shallow water; some probes do not respond in a linear fashion in very shallow water, and some do not produce continuous results when fully emerged from water, which presents problems for studies of phenomena such as water on deck.

The results from a survey carried out by the 22nd ITTC Loads and Responses Committee (1999) on the usage of wave measurement technologies amongst 40 ITTC members are shown in Table 1. Naturally many institutions will use more than one technology.

Resistance	19
Servo	16
Capacitance	11
Acoustic / Ultrasonic	6

Table 1 Usage of wave measurement technologies by ITTC members

5.2.1.2 Uncertainty of Intrusive Wave Measurement Systems

Bouvy *et al.* (2009) carried out a thorough investigation of the measurement uncertainty for resistance, capacitance, servo and ultrasonic wave measurement systems by moving probes through four displacement sequences in still water, both upwards movements and downwards. They estimated the uncertainty due to linearity, reproducibility, reversibility, and positioning error as shown in Table 2. Reversibility refers to the differences observed between cases when probe is entering and emerging from the water, due to wetting and unwetting and/or meniscus effects.

Probe type	Measurement Uncertainties (mm) due to:				
	Linearity	Reproducibility	Reversibility	Positioning	Uncertainty (U95)
Resistance	0.4	0.9	0.9	0.12	1.5
Capacitance	0.7	0.3	1.5	0.12	1.9
Servo	0.9	0.8	1.5	0.12	2.1
Ultrasonic	0.3	0.4	0	0.12	0.6

Table 2 Measurement uncertainty for intrusive wave measurement systems (Bouvy *et al.*, 2009)

It can be seen that relative uncertainty levels with these probes are quite large if small waves are of interest. Day *et al.* (2011) point out that estimation of uncertainty based on static calibration neglects some components of error which will increase uncertainty in practical testing; these include issues such as run-up, ventilation and wave scattering for intrusive resistance or capacitance probes. Martins *et al.* (2007) studied the impact of dynamic vertical oscillation in still water on measurements made by capacitive, resistance and (submerged) ultrasonic probes. Results showed that both amplitude and phase of output signals from resistance and capacitance probes depended upon frequency in the range from 0-3Hz. Phase variations from resistance probes were particularly significant.

5.2.1.3 Ultrasonic Systems

Since the survey of 1999, there has been increasing interest in the use of airborne ultrasonic probes, mounted above the water surface with the beam pointing downwards. Key performance parameters for ultrasonic probes include the maximum and minimum measurement distances, the beam angle, which determines the size of the acoustic footprint, and the update rate.

Bouvy *et al.* (2009) compared the results from intrusive probes with those from a sophisticated ultrasonic device incorporating three sensors, each with beam angle less than 3 degrees and update rate of 100 Hz. An additional sensor was used to measure the speed of sound and thus eliminate the need for calibration. Results showed that the ultrasonic probe demonstrated lower uncertainty than the resistance, capacitance and finger (servo) probes when the effects of reversibility (differences between moving probes in and out of the water) and reproducibility are included, as shown in the table above.

In comparison, Day *et al.* (2011) estimated a 95% uncertainty due to linearity of a single-sensor ultrasonic probe with a beam angle less than 3 degrees and update rate of 75 Hz. Static calibration tests carried out in calm water yielded 95% uncertainty value due to linearity only of 0.76 mm, compared to the value for a resistance probe of 0.56 mm; these figures exclude uncertainty due to reversibility, reproducibility and positioning error. They discuss the neglect of dynamic effects on uncertainty for ultrasonic probes due to spatial averaging at wave peaks and troughs related to the finite size of the acoustic footprint for the ultrasonic probe. This issue is also discussed by Richon *et al.* (2009).

Ultrasonic probes have been shown to work particularly well when water surface is roughened, increasing diffusive reflection, for example by capillary waves or in cases of white water in the stern wake of a high-speed ship. Fu and Fullerton (2009) show results of measurements of transom wave-breaking for NSWCCD model 5673 using an ultrasonic probe with beam angle of 15 degrees and sampling rate of 20 Hz. Results demonstrate that the probe works well in the complex unsteady multiphase flow. Bouvy *et al.* (2009) show a comparison between measurements in a high-speed ship wake made by an acoustic probe and a servo probe, demonstrating that the servo probe identifies many spurious peaks which were not found in the measurements using the ultrasonic device.

One disadvantage of ultrasonic probes is the tendency for signals to "drop out" when the echo is not picked up by the receiver. Bouvy *et al.* (2009) describe a sophisticated technique for reconstructing drop-out regions.

5.2.2 Emerging Techniques for Wave Measurement in Test Facilities

5.2.2.1 Bottom-Mounted Ultrasonic Systems

An alternative approach to the use of ultrasonic systems is to mount the sensor underwater, typically on the bottom of the tank. This configuration has the particular advantage of allowing ship models to pass over the point of measurement without any interference. Bouvy *et al.* (2009) describe the development of a grid of underwater ultrasonic sensors for the Duisberg Shallow Water Towing Tank.

A different bottom-mounted ultrasonic system described by Fullerton and Fu (2008) and Fu *et al.* (2009) is the Acoustic Wave and Current Profiler (AWAC) system. This device is based around a conventional three-beam Acoustic Doppler Current Profiler (ADCP), a bottom-mounted ultrasonic system primarily used for current measurements. A fourth acoustic beam is oriented vertically to measure water surface elevation. These devices have a relatively low sampling rate (typically 4Hz) and are thus restricted to measurements of long period waves. They are widely used for field measurements of wave and tidal environments and less commonly used in laboratory testing. In these studies the device was successfully used in conjunction with airborne ultrasonic probes and laser systems to measure the wave profile on a longitudinal cut.

5.2.2.2 Optical-Based Point Measurement Systems

Over the past twenty years a number of studies have examined the use of optical systems to measure water surface elevation at discrete points, based on a variety of techniques. Many of these are aimed at applications rather different from ship model testing. For example Martinsen and Bock (1992) used a bottom mounted laser firing vertically upwards to measure small ripples, such as capillary waves, on the water surface. As the beam passes through the air-water interface, refraction at the water surface results in a beam deflection angle that is proportional to the surface slope. The deflected beam is collected by a lens and focussed onto a photo detector.

In more recent years several studies have examined the use of optical systems to measure wave elevation at discrete locations. These are generally based on optical triangulation and are similar in concept to laser rangefinders. Systems use a CCD camera to capture the image of a laser aimed at the water surface. The image typically consists of a line; one end of the line represents the intersection of the laser beam with the water surface, while the other represents the reflection of the light from the bottom or side of the tank. Image processing is used to identify the location of the end of the line at the water surface in terms of pixel location on the CCD. Calibration is achieved by moving the camera and laser vertically relative to still water and yields the relationship between the pixel location and

water surface elevation. Due to perspective effects the calibration is somewhat non-linear.

Atsavapranee *et al.* (2005) and Carneal *et al.* (2005) describe the development of a system described as Global Laser Rangefinder Profilometry (GLRP) which uses a large array of low-power (3.5-15mW) lasers to measure wave elevation at discrete points on the water surface. The technique utilizes an area-scan CCD camera to image the points of intersection of the laser beams on the surface, which is enhanced with fluorescent dye to improve image contrast. Figure 24 shows a schematic of a typical test setup. Figure 25 shows a superposition of five images of the laser spots, taken in calm water at five different water elevations, illustrating the shift in the apparent positions of the spots with changes in water surface elevation. Particular emphasis was placed on the identification of the individual points and the correlation with calibration data to obtain local wave elevation at each discrete position. The approach was compared with ultrasonic measurements, and was shown to measure peak-to-peak wave heights around 5% higher, presumably due to the spatial averaging of the sonic beam at wave peak and trough. Uncertainty analysis indicated a measurement uncertainty of around 1.6 mm. Figure 26 shows an example of a GLRP measurement of a large-amplitude oblique wave at 400 discrete points, performed in the Maneuvering and Seakeeping Basin (MASK) at NSWCCD.

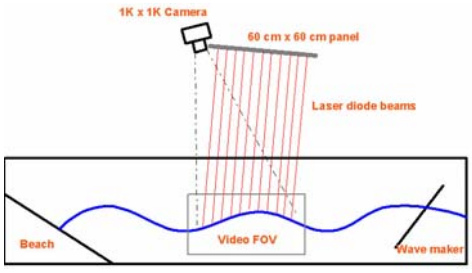

Figure 24 A GLRP measurement setup

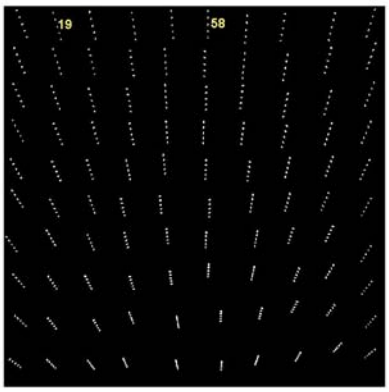

Figure 25 GLRP calibration: superposition of five surface displacement calibration images taken in calm water at five water elevations

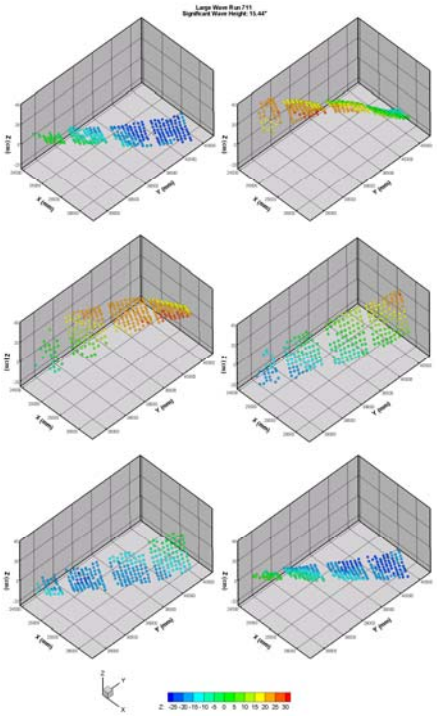

Figure 26 Example of GLRP measurement in the MASK Basin at NSWCCD of a large-amplitude oblique wave (Carneal *et al.*, 2005)

Recently, the GLRP technique has been used to quantify the three-dimensional wave field in an investigation of various means to generate large-amplitude wave groups and single extreme waves (Bassler *et al.*, 2008). Figure 27 compares measurements from a sonic probe with one GLRP point measurement (out of 200). The kinematics of the large-amplitude

wave groups were also measured using PIV by Minnick *et al*. (2011). Figure 28 illustrates an example of an instantaneous PIV measurement of the wave orbital velocity, and Figure 29 illustrates the flow field within a wave group. The top plot is the wave height time history of the wave group at one location in the basin, and the bottom plot is the time history of the velocity measurement along a vertical line underneath wave height measurement location (waves are moving right to left). The *x*-axis has been compressed for visualization purposes and therefore, the relative steepness among waves has been distorted.

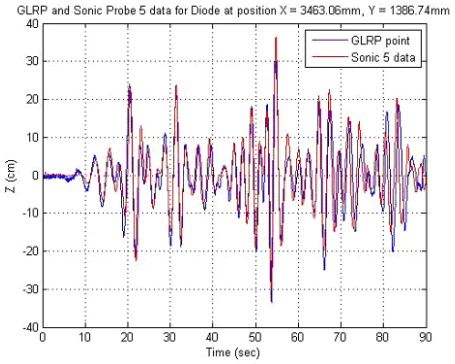

Figure 27 Comparison between GLRP and sonic probe in the measurement of a large-amplitude wave group (Bassler *et al*., 2008)

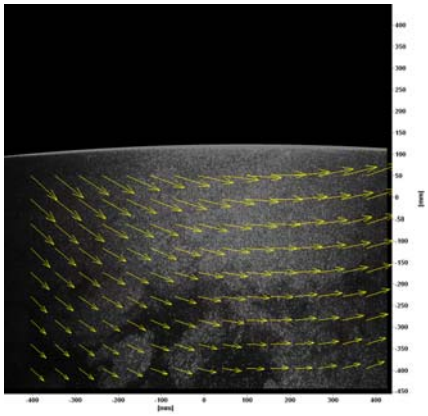

Figure 28 Example PIV image and the associated wave orbital velocity from Minnick *et al*. (2011)

Richon *et al.* (2009) describe the development of a single point measurement system based on the principle of a laser rangefinder for the B600 Towing Tank in Val de Reuil, France. The system uses a high-power laser pointing vertically downwards at the water surface with a 100-Hz CCD camera recording a narrow image of the laser spot and the underwater beam with resolution of 1392 x 64 pixels. The system achieved an accuracy of better than +/- 1mm in a calibration tank. The laser system was shown to predict RMS wave heights around 3-5% larger than those measured using an ultrasonic system, a result consistent with the findings of Atsavapranee *et al*. (2005). Payne *et al.* (2009) describe the development of a system using a moderate power laser (200mW). Using a cubic calibration curve, the uncertainty due to calibration was shown to be better than 0.5 mm. Results for waves of amplitudes 25 mm and 50 mm with frequency 1.0 Hz were compared with results gained from a resistance-type probe. It was observed that the optical probe predicted sharper peaks and flatter troughs than the resistance-type probe, closer to the results from a fifth order Stokes wave model.

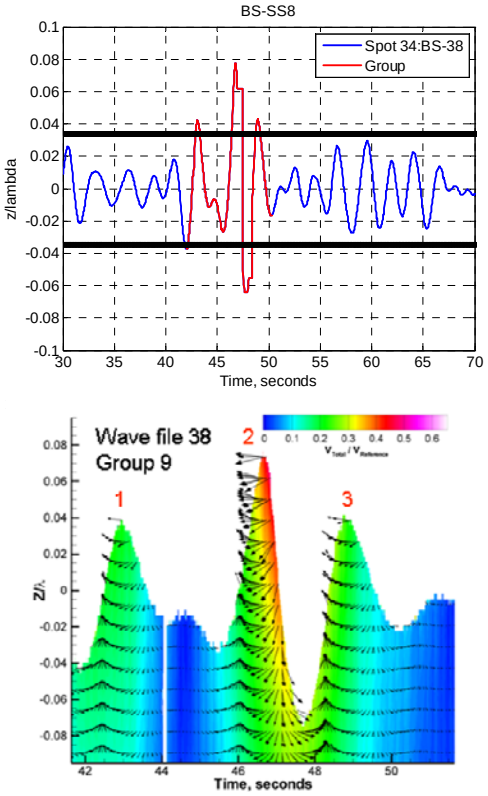

Figure 29 Wave kinematic measurement with PIV from Minnick *et al*. (2011)

Day *et al.* (2011) describe the development of a low-cost single-point system using a 200mW laser pointer and a low-cost consumer video camera. Calibration uncertainty was shown to be around 0.6 mm when a quadratic calibration was used. Similar to the three previously-mentioned papers, results from the laser probe for RMS wave height in random waves were shown to be larger than those measured by resistance or ultrasonic probes; even after a dynamic correction had been made based on single frequency waves. The differences were particularly noticeable at the peaks of the waves. Some phase differences were also identified between the laser measurements and those from resistance and ultrasonic probes.

5.2.2.3 Light-Sheet Line Measurement Systems

An alternative to the point measurement system is to use a light sheet to illuminate a line on the water surface. In some cases the light sheet is projected down at the surface, in others the light source is immersed and projected upwards. A CCD camera captures the image of the line, and image processing techniques based on segmentation procedures and edge or contour detection are used to identify and track the wave profiles. Calibration is often based on the use of a calibration grid, allowing quantitative measurement. In many cases techniques have been applied in relatively small tanks or flumes, avoiding some of the challenges of large test facilities.

Yao and Wu (2005) describe two applications of such a technique in a small wave-current flume. One version used a 5W laser to generate a thin light sheet projected downwards onto the water surface. Image contrast was enhanced by use of fluorescent dye. The second version, suitable for larger fields of view, employed a halogen light source shining through the glass wall at the front of the flume and reflected from a panel mounted on the back of the flume. A gradient vector flow (GVF) "snake" was used to track the surface profiles automatically. Results successfully capture fast-deforming steep surface wave profiles such as plunging breakers, and breakers impacting cylinders. Mukto *et al.* (2007) describe a particle-image based technique for measurement of small-scale wind-generated wave profiles in a wind-wave tank simultaneously with PIV measurements. Water was seeded with hollow glass spheres. A laser light sheet was projected upwards from the bottom of the tank, and images captured on a 2MP digital video camera at up to 60Hz. A detection algorithm referred to as the variable threshold method was used to capture the free surface profile.

A number of studies have reported the use of similar techniques in towing tank applications. Furey and Fu (2002) describe an early implementation of the QViz (Quantitative Visualisation) system which used a high-power (5W) laser to create a light sheet normal to the water surface. A 640x480 digital camera system recorded images of the intersection of the light sheet with the water surface, and a variety of image processing techniques were explored to identify the position of the water surface. Images are calibrated relative to still water conditions; hence, the results give wave elevation along a line. In some conditions fluorescent dye is used in conjunction with narrow band-pass filters to improve image contrast. Comparisons were made with data from finger probes in a small wave flume, with turbulence induced by a breakwater with mixed success. The authors concluded that the method was most suitable for slowly varying flows, flows with high frequency small amplitude variations or steep surface flows. Developments and subsequent applications of the system are described in Rice *et al.* (2004), Fu *et al.* (2005) and Fu *et al.* (2009). Field application of the system to measure the bow and stern waves of a full-scale ship at sea is described in Fu *et al.* (2006). A low-cost implementation of a similar technique is described by Calisal (2009) and Calisal *et al.*

(2011) using extensive floating seeding to increase image contrast.

Perelman *et al.* (2011) describe the application of a laser light sheet approach to ship wave measurement in the B600 test tank in France. The laser sheet is projected upwards from the bottom of the tank, and a series of five video cameras are mounted close to the water surface recording the intersection of the sheet with the free surface. Image processing techniques based on grey level weightings allow determination of the surface profile with sub-pixel precision. With the light sheet arranged transversely, the 2D wave field can be obtained as the ship passes. A comparison made along a longitudinal cut with measurements from an ultrasonic wave probe show good agreement. The authors identify particular challenges of this technique in breaking waves, such as transom flows, where no clear image of the surface can be obtained.

5.2.2.4 2D Optical Measurement Techniques

A variety of techniques have been explored to measure waves over an area rather than along a line or at a discrete point. A stereo–photogrammetry technique developed for measuring temporal evolution of three dimensional wave characteristics described as the *Automated Trinocular Stereo Imaging System (ATSIS)* is described by Wanek and Wu (2005). The system uses three CCD cameras to capture three independent stereo pair images allowing accurate estimation of depth of a scene and reducing the chances of image mismatches. A two-step calibration procedure is proposed; the first step (described as interior calibration) corrects for lens distortion and identifying the image-center coordinates for each camera, whilst the second step (exterior calibration) determines the focal point and camera orientation in the global coordinate system. In this study, the field measurements were made outdoors, in light conditions yielding high contrast images. Results were validated by comparison with a capacitance wave probe, showing good agreement.

Application of the technique in tank tests is discussed by Stansberg *et al.* (2009). Difficulties identified in the use of the technique in laboratory conditions include problems with matching images due to reduced contrast, use of "point" light sources, and reflections from building or carriage structures. A variety of suggestions were made for improving the technique, including use of seeding and underwater lighting.

Perelman *et al.* (2011) describe the attempts made to improve the technique at the B600 towing tank in France. Efforts were concentrated on providing texture to the surface to provide features which could allow matching. Roughening the surface using a fan to generate capillary waves was unsuccessful; however, the use of floating seeding generated better results, and successful matching was performed using two cameras. Validation was performed by comparison of a measured time history with data from an ultrasonic probe. Agreement was good; however, the optical technique predicted wave height 4% greater than the ultrasonic probe. This discrepancy is similar to that found in point measurements by Atsavapranee, *et al.* (2005), Richon *et al.* (2009), and Day *et al.* (2011).

Grid projection techniques represent another different approach for surface-wave measurements. Kanai (1985) describes a technique based on the measurement of the deformation of a grid pattern projected onto the water surface from above. Sanada *et al*. (2008) measure the instantaneous 2D wave field around a ship model by projecting a colour-coded line pattern onto the water surface. The lines on the wavy surface are matched with the lines on the still water surface in order to obtain the surface slopes. The wave slopes in x and y directions are used to estimate the strengths of a series of point sources using potential flow theory, and in turn the source strengths are used to reconstruct wave heights. A comparison

with measurements made using capacitance probes indicates maximum error of around 1 mm for waves 10 mm in height.

Fu *et al.* (2009) describe the use of a LiDAR (Light Detection and Ranging) system for measurement of transom waves behind a large model. LiDAR is a scanning time-of-flight system measuring the time of return of infrared pulses to measure water surface elevation over a 2D field. In the system used, the sampling rate was 20Hz, and the resolution of the system is around 20 mm; consequently, the system is more commonly used in field trials, or very large scale model measurements.

5.2.2.5 Other Systems for Surface Wave Measurement

Kaminski and Bogaert (2009) and van den Bunt and Kaminski (2009) describe an unusual technique for capturing the highly rapid evolution of the shape of the jet of 2D plunging breakers impacting upon a wall in the Delta Flume. Conventional optical techniques were unable to see the lower surface of the jet from above. A system described as iCAM (impact Capturing Matrix) was developed. These consisted of a series of small optical sensors which were designed to register whether their outer surface was in water or in air. These sensors could be sampled at up to 15 kHz. A 40 x 16 grid of the sensors was mounted in a vertical strip adjacent to the flume wall, effectively forming a pixelated image identifying the regions which were in contact with air or water. This measurement was then combined with data obtained from a calibrated high speed video system to capture the wave front progression in the 6-m section of the flume prior to the end wall.

Geerts *et al.* (2011) describe the development of a low-cost technique for measurement of dynamic waterline on a ship model using fluorescent paint and UV light. The model is photographed using a high-resolution digital still camera. A projected Cartesian mesh painted on the model is used to correlate the warped image with a projected side view of the ships hull, avoiding the need for multiple camera stereo-vision systems.

Fu *et al.* (2009) describe the use of an impedance probe designed to infer the void fraction in bubbly flow to measure void fraction in breaking transom waves.

5.2.2.6 Measurements in Stratified Fluids

A number of studies have been carried out at CSSRC investigating the fluid mechanics of internal waves in stratified fluids. Internal waves have long period and wave length; although the flow velocities induced by internal waves is very low, they can propagate far away, and even penetrate to the free surface. PIV was used to measure the flow field generated by an underwater moving body in CSSRC's stratified fluids tank. The CCD has the resolution of 1600x1200 pixels, and the viewing window is about 1000mm×750 mm, so several periods of waves can be captured. Three kinds of seeding particles were used to measure different horizontal planes. One is tree pollen with the density about 950 kg/m^3; the other two are polymers with density about 1030 kg/m^3, and 1045 kg/m^3. The pollen particles floating on the free surface are illuminated by a system of lamps. Figure 30 illustrates the surface flow induced by the internal waves. The polymer particles in the bulk fluid were illuminated by a laser sheet at different horizontal planes for velocity measurement at different elevations.

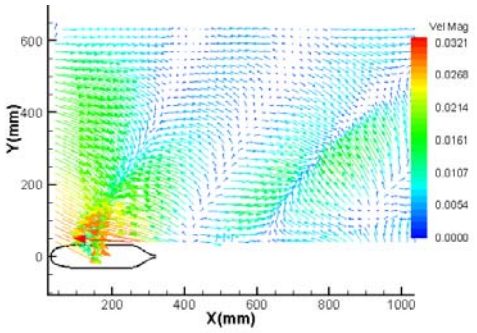

(a) Vectors of flow velocity

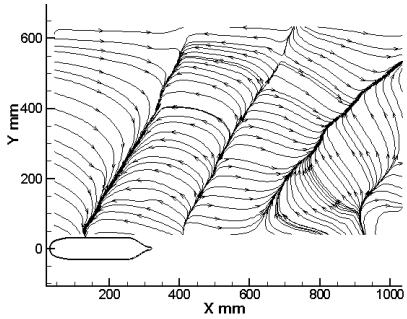

(b) streamtrace of flow field

Figure 30 PIV measurements showing surface flows induced by internal waves generated by an underwater body moving in stratified fluid

An optical refraction technique was also used to measure small surface waves induced by internal waves in the stratified tank. Figure 31 shows a schematic of this method. A benchmark target was fixed on the transparent bottom of the tank. The light propagating through the free surface was refracted and recorded by a CCD camera. When the free surface is disturbed, the free surface slope becomes irregular, and the image of the benchmark target is distorted. Comparing the distorted and undistorted image allows the reconstruction of the free surface slope. Based on the integral of the surface slope, the surface wave height can be acquired. Figure 32 shows a distorted image of the benchmark target and the measured surface waves. Because the stratified fluids were mixed by the turbulence wake of the moving body, the image in the wake of the moving body became unclear and is not well measured by this optical method.

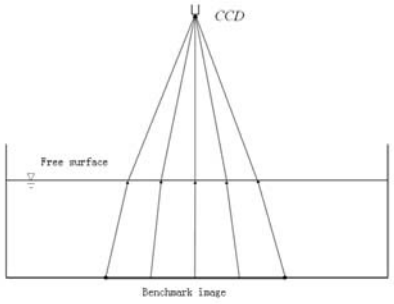

Figure 31 Schematic of the optical measurement of small surface waves

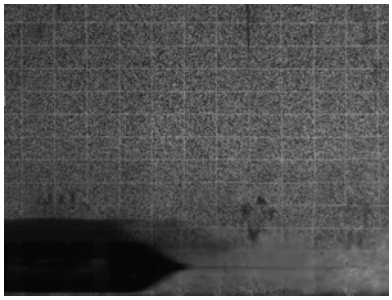

(a)

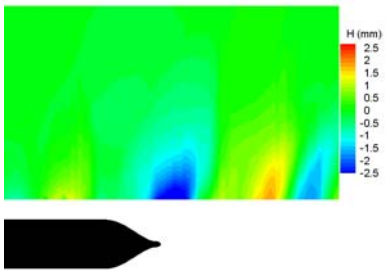

(b)

Figure 32 Distorted reference image (a) and surface wave (b)

6. CURRENT AND FUTURE WORK

The state-of-the-art review in Section 4 provides an overview of the recent and current applications of detailed flow measurements in various aspects of hydrodynamic research in different test facilities. Furthermore, it highlights the fact that many practical issues remain and much further work needs to be performed to facilitate the adoption of these techniques in the mainstream ITTC community.

6.1 Practical Issues for PIV/SPIV Applications

The committee recognizes that a practical guideline on the application of PIV/SPIV in large-scale facilities would be highly valuable for the ITTC community. While conceptually worthwhile, the development of such a guideline is complicated by the fact that potential applications for PIV are so wide ranging and would concern practitioners of various levels of knowledge and experience. The present section outlines some considerations and practical information from

preliminary work by the committee, which would hopefully lead to the development of a more comprehensive best-practice guideline in the framework of the 27th ITTC Conference.

The typical hardware for a PIV or an SPIV measurement consists of one or two digital cameras, a light source (typically a pulsed laser), light sheet forming optics, and a synchronizing unit, as shown in Figure 33.

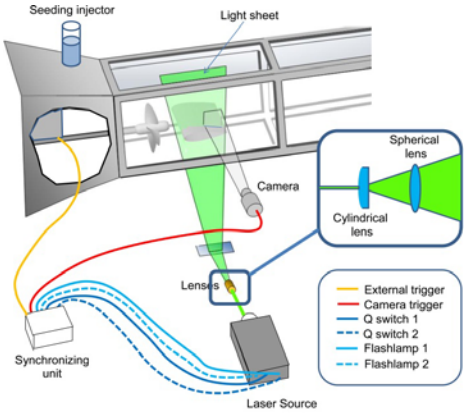

Figure 33 Overview of a PIV setup

PIV measures the flow velocity indirectly by measuring the displacement of seeding particles within the fluid. This characteristic makes the choice of particles a critical component of a PIV system. Seeding particles must closely match the fluid properties and provide efficient light scattering. In addition, the distribution of seeding should be as homogenous as possible. Figure 34 shows an image of a suitable seeding distribution. A simple rule of thumb is to gradually seed the water until an adequate distribution is reached (at least 10 particles per interrogation area are required on average). Flow seeding is normally performed by dedicated rake devices, suitably placed far upstream of the experiment to avoid any flow disturbance in the measurement area. In towing tank applications, such problems can be overcome by placing the rake downstream of the measurement area and seeding the flow during the return run of the carriage.

Figure 34 Example of a suitable seeding distribution (crop of 128x128 px^2)

In a PIV experiment, the light source acts as a photographic flash for the digital cameras which record the light scattered by the seeding particles. A PIV record typically involves an image pair produced with two laser pulses recorded onto two consecutive camera frames. The requirements for a laser system are directly related to the size of the measurement area. In most tow tank institutions, ship model length ranges from 3 to 8 m, and propeller diameter ranges from 130 to 350 mm. These dimensions provide the basic requirements for the size of the measurement area. A typical PIV application in water requires an energy density ranging from $5x10^{-4}$ to 10^{-3} mJ/mm^2 (for light sheet thickness of 1mm seeded with 10 µm hollow glass particles). This allows a rough estimation of the laser energy to be supplied once the extent of the field of view has been established. For instance, in most towing tank and hydrodynamic applications, a 200 mJ laser is normally adequate to investigate areas in the range 100x100 mm^2 to 500x500 mm^2.

Besides the laser energy, other relevant aspects in the choice of a laser source for a PIV application are the repetition rate and the size and weight of the laser. The repetition rate of the laser pulses should match the exact camera frame rate or its multiples, in order to maximize the frame rate of the PIV acquisition. For this reason, the use of lasers which can

handle a range of variable repetition rate is recommended. The size and weight of the laser system are important factors that determine the ease of equipment handling in the setup stage.

Key considerations to be made in the choice of a PIV camera are the resolution of the sensor and the frame rate. Resolution and frame rate are interrelated by an inverse relationship (higher resolution cameras typically have lower frame rate); and thus, a trade-off usually has to be made, considering i) the type of fluid flow, ii) the required spatial resolution, and iii) the required acquisition run length. A typical value of suitable resolution in a PIV measurement ranges between 50 and 300 μm/pixel.

The trend towards higher resolution for PIV cameras and consequently increased quantity of image data has made data management a critical issue in PIV. The memory space S of an instantaneous PIV/SPIV acquisition (one or two image pairs), acquired by camera(s) with P mega pixels and saved in a Q bit format is:

$$S = N \cdot [P \cdot (Q/8)] \quad \text{MBytes} \qquad (1)$$

where $N = 2$ for 2C-PIV and $N = 4$ for SPIV. Therefore, the amount of data for the whole experimental campaign is obtained by multiplying the result of (1) by the number of instantaneous acquisitions. In a typical PIV-SPIV campaign, usually hundreds of Gigabytes of images have to be managed. Normally the process of saving, restoring and data processing are time-consuming, and a rough rule of thumb is that data acquired in one day of towing tank experiments require at least 5 days to be processed, with currently available computer technology (3 Ghz multicore- multiprocessor PC) and state-of-the-art PIV algorithms.

In a PIV experiment, the quality of the final results depends largely on how visible and well identifiable the seeding particles are within particle images. Therefore, it is critical to avoid, or at least, minimize any light reflection from the model and the background, once a homogeneous seed distribution is obtained. In this regard, a common practice is to apply opaque-black paint to the area being illuminated or manufacture that section out of transparent material such as Perspex (Figure 35). The use of a black cover to mask any background object in the field of view of the PIV camera is also strongly recommended. Alternatively, image pre-processing techniques may be used if the experiment does not allow background masking (Figure 36).

Figure 35 Use of Perspex made objects to avoid light reflection (Felli *et al.*, 2010)

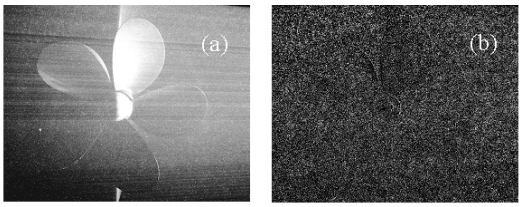

Figure 36 Image preprocessing: a) original image, b) pre-processed image

For small setups, when the volume of the flow to be seeded is small, it is possible to use very costly fluorescent particles which absorbs the incident laser light and reemits a fluorescent output at a different wavelength. In such a manner, it is possible to reduce the effect of surface reflection by using a dedicated interferential filter in front of the camera objective lens to block out the laser wavelength of the surface reflection and pass the fluorescent wavelength of the seed particles.

In PIV, particle displacements are measured in the image plane and thus, represent a magnified/scaled measure of the physical displacement. The calibration process provides

the measure of the mapping function by which the image plane is mapped into the physical plane. For conventional PIV the variation of the mapping function over the field of view is usually negligible because the image-plane is parallel to the light sheet. It is, therefore, reasonable to assume that the mapping function is constant over the entire image. The value of the magnification factor is determined by imaging a reference object with known length L_o in the object plane. The magnification factor M is given by L_o / L_i, where L_i represents the length of the reference object in the image plane, measured in pixels. In the image plane, the uncertainty in the measure of the reference length should be minimized as much as possible. Care should be taken to position the reference object in the plane of focus and the use of easily identifiable reference marks is recommended.

The issues discussed in this section are among a few of the many considerations that would have to be addressed in the conduct of high-quality PIV/SPIV measurements in large-scale facilities. Many practical issues, related to the complex setup (underwater housings, mounting support, system alignment, calibration, light delivery, seeding, etc), make the applications of PIV/SPIV still a challenge for wide-scale use in general ship hydrodynamics investigations. The committee hopes to address these and other issues in a more details in the context of a best-practice guideline for the 27th ITTC conference.

6.2 Benchmark for the Verification of PIV/SPIV Setup

Another area that the committee considers critical towards facilitating the adoption of detailed flow measurements is the availability of benchmark data for the purpose of verifying the quality of the measurement setup. The primary purpose of using these benchmark cases is to ensure that the measurement system and the configuration of the cameras and light sheet are meeting specifications.

Recognizing again that potential applications for PIV are wide ranging and would concern practitioners of various levels of knowledge and experience, the committee is exploring two distinct benchmark cases. The first case utilizes a two-component PIV system on a simple 2D geometry. The second uses an SPIV system on a more complex 3D flow field.

6.2.1 2C PIV Setup Benchmark

Possible situations in which the 2D benchmark may be suitable are:

a) An organization may be acquiring a PIV system and would like to evaluate it on a simple known flow.

b) An organization has acquired a PIV system and is in the process of learning the system or need to train test personnel in using the system.

c) An organization needs to evaluate the performance of an existing PIV system to ensure that it meets industry standard and customer performance criteria.

A simple 2D benchmark case, based on the experiment performed by Hudy and Naguib (2003), is proposed for the purpose of the verification of the setup of 2D PIV systems. A good benchmark case should include typical flow features found in marine hydrodynamics such as flow separation and vortex generation. At the same time, it should be easy to set up and should not be very sensitive to flow conditions such as small change in Reynolds number or small manufacturing imperfection of the model. For these reasons, a separating-reattaching flow around a splitter plate with a fence was chosen as a candidate. Figures 37 and 38 illustrate the geometry and the flow. The fence height above the splitter plate (h_f) is 10 mm, and the total fence height ($2H$) is 40 mm. In order to assure two-dimensional flow, both ends of the plate and fence should either span the entire width of the test section or be

attached to end plates of sufficient size. The Reynolds number based on the fence height and the free stream velocity is 8000.

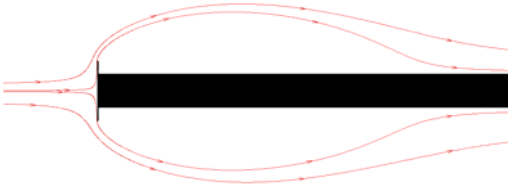

Figure 37 Flow around splitter plate with fence

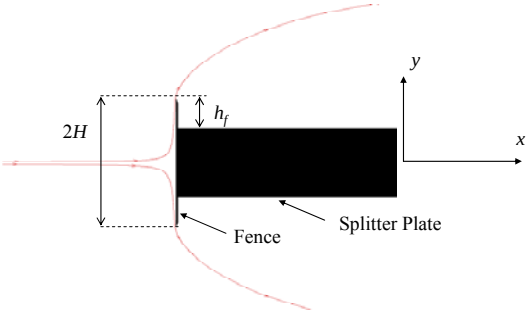

Figure 38 Geometry of the 2D benchmark

The influence of flow parameters and model geometry on the flow field was investigated using 2D RANS simulations with the commercial CFD code Fluent. Various tip geometries were examined, and the results show that the geometry illustrated in Figure 39 to be suitable. The front face of the fence is kept flat and perpendicular to the flow axis to create a stagnation flow before it detaches from the sharp tip. Results show that if the backside is bevelled less than 45 degrees, the flow is not sensitive to small variation in the bevel angle or the fence thickness. Velocity vectors near the fence are shown in Figure 40.

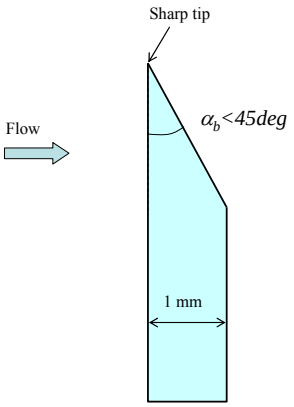

Figure 39 Detailed geometry of the fence

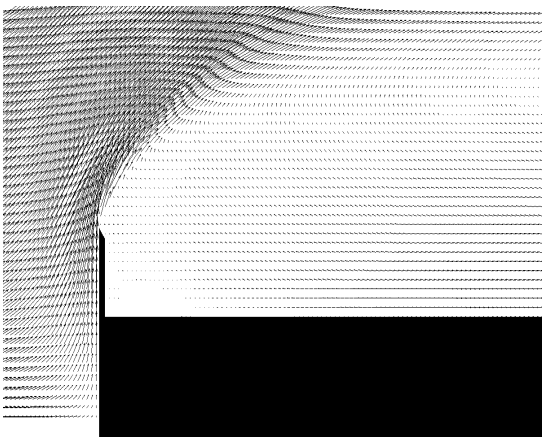

Figure 40 Velocity vectors around the fence

RANS simulations at twice and half of the target Reynolds number of 8000 were carried out and confirmed that the reattachment location does not change significantly with Reynolds number, making the flow relatively insensitive to small variation in tunnel speed and water properties. The influence of the splitter plate length was also investigated. Because of the pressure gradient at the end of the splitter plate, the reattachment location was found to be weakly dependent on the splitter plate length. However, when the splitter plate length is more than 100 times the fence height above the splitter plate (h_f), the effect of the splitter plate length was found to be negligible.

This preliminary assessment is based on 2D steady RANS. More detailed computations, possibly with URANS or LES, and test data from different facilities are needed in order to finalize the specifications of the 2D benchmark.

6.2.2 Stereo PIV Setup Benchmark

The use of SPIV is widely expanding in many fields of naval hydrodynamics. Various ITTC organizations are recently investing in this maturing technique, which is beginning to make possible industrial-type measurements with a drastic reduction in time and cost. This trend has introduced new critical issues related to the assessment of the SPIV setup for

applications in large-scale facilities. There is a clear need to devise and share a specific benchmark by which researchers in various organizations can exchange know-how's and assess the quality of their setup and procedures.

A piercing surface flat plate operating at incidence is selected as the test case for SPIV benchmarking. This test case was devised by the European Network of Excellence Hydro Testing Alliance (HTA), and many HTA members have participated in its assessment. Recently, the Detailed Flow Measurements Committee has engaged in discussions with the HTA JRP1 working group to explore possible collaboration in areas of common interests. As a result, the committee has performed an initial evaluation of the 3D benchmark case. Specifically, a good benchmark test case:

- should be representative of the major critical issues of SPIV measurements in towing tanks or circulating water channels, such as high velocity gradients, surface effects, presence of air bubbles and reflections;
- should represent a simple and cheap experimental setup that can be adapted to the multitude of facilities;
- should be defined by detailed and unambiguous specifications to assure high repeatability tests among partners;
- should be easy to set up in a short period of time (about 1 hour or less) during any test campaign in a towing tank or a circulating water channel;
- should require no more than 1 or 2 carriage runs to obtain measurements

The primary value of the benchmark arises from the ability for different organizations to share images and velocity data on the same experiment performed in various facilities, using the same basic technique but with some variation in specific approaches. It is assumed that unique requirements of each facility may dictate some differences in procedures. Each organization would be free to approach the test case in its own way, for example reflections can be minimized using special paints, using fluorescent seeding particles or special filters.

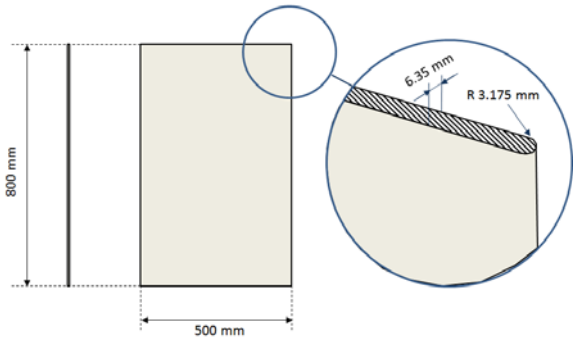

Figure 41 Flat plate geometry

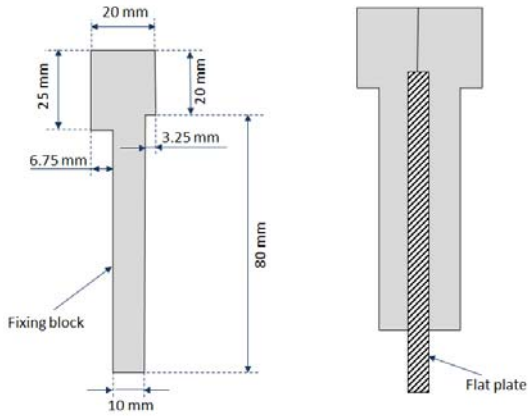

Figure 42 Flat plate fixing blocks

Figure 41 shows a representative sketch of the piercing surface flat plate. The plate is a steel rectangular plate measuring 800 mm (L) x 500 mm (W) x 6.35 mm (H). Both leading and trailing edges of the plate have a round edge of 3.175 mm radius. The plate experiences some deformation when operates at incidence. It is therefore important to assure the plate deformation be repeatable in all the benchmarking exercises. In this regard, the benchmark case also specifies the geometry of the anchoring system, which consists of aluminum blocks held together by screws, as detailed in Figure 42.

Two experimental configurations have been proposed to fit the standard characteristics of

towing tanks and circulating water channels, as documented in Table 3.

	Towing tank	Circulating water channel
Plate dimensions (L x W x H) (mm)	500 x 800 x 6.25	500 x 800 x 6.25
Speed (m/s)	0.4	2
Angle of incidence (deg)	20	5
Tip-free surface distance (mm)	300	300

Table 3 Configurations for towing tank and circulating water tunnel

Two cross planes in the near tip region of the flat plate (Figure 43), located 100 mm in front (plane P1) and behind (plane P2) of the trailing edge, have been identified for the benchmarking exercise. An upstream cross plane far enough from the leading edge also has been considered to survey the undisturbed velocity field. The field of view is rectangular (at least 200 mm high by 300 mm wide) and is situated on the suction side of the incident plate. The dataset should consist of at least 128 instantaneous three dimensional velocity fields. For the sake of maintaining a homogeneous data format among participants, mean velocity fields should be provided according to the following order: X (mm), Y (mm), Z (mm), U (m/s), V (m/s), W (m/s). The origin of the reference system has been set at the trailing edge of the plate tip, with the X axis aligned to the free-stream direction, the Z axis vertical and the Y axis horizontal and oriented from the low to the high pressure side of the plate.

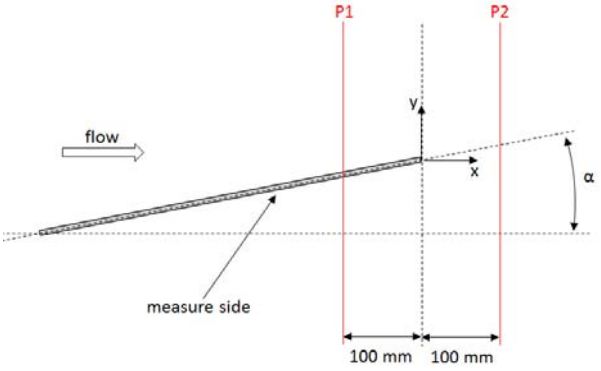

Figure 43 Measurement planes

Instantaneous images from the left and right cameras in tiff or bmp format, instantaneous velocity fields from the left and right camera and after the stereo reconstruction, calibration images, datasheet with the mean velocity fields as previously specified, testing and processing information (e.g., left and right camera arrangement, set up specifics, processing and stereo reconstruction techniques and parameters) are requested to be supplied by each of the participants.

The committee hopes to organize a detailed evaluation of this benchmark through participation by the larger ITTC community in the framework of the 27th ITTC Conference.

6.3 Discussions on Error Sources in PIV/SPIV Measurement

The 25th Specialist Committee on Uncertainty Analysis published procedure 7.5-01-03-03 on the uncertainty assessment of PIV that is both up-to-date and compliant with industry standards in regards to uncertainty analysis methodologies. Although the current procedure is very comprehensive in its coverage of error sources due to the PIV measurement system itself, sources of bias and random uncertainties due to the particulars of the flow (velocity gradients within the flow, out-of-plane particle motion across the laser sheet) and test-specific issues (such as seeding density and non-uniformities, particle image size, and laser glares on model) were not addressed. The present section provides a

discussion of some of these error sources that should be addressed further and quantified in future updates of the procedure.

6.3.1 Particle Displacement Uncertainty

The uncertainty in the estimated particle displacements determined by PIV image analysis includes both precision and bias errors. Each velocity component is computed from the displacement estimate using the following relationship:

$$V_i = \Delta s_i * M / \Delta T \text{ where } M \equiv L_o / L_i.$$

The laser pulse delay, ΔT, is assumed known with a specific uncertainty and M is the image magnification, defined as the ratio of L_o (the object calibration length in test units of length) and L_i (the image calibration length in pixels). The uncertainty in M is related to the calibration process. The current PIV uncertainty guide provides procedures for defining the uncertainties in ΔT and M. The particle displacement, Δs_i, is typically measured as a statistical mean particle displacement of N number of particles in a small interrogation region (IR) of the two double-pulsed images. Many algorithms are available to estimate the mean displacement in an IR ranging from tracking individual particles, to FFTs, to direct spatial cross-correlation. The latter two are the most commonly used. In either case, the displacement in pixels is estimated using the location of the cross correlation peak. Several other important factors, such as resolution error of the displacement engine, peak locking, perspective distortion, and image spatial resolution, may contribute to displacement uncertainty.

6.3.2 Contribution of Displacement Engine Resolution to Displacement Uncertainty

The resolution of the PIV correlation algorithm is but one component of the total uncertainty in the displacement measurement. The minimum possible displacement resolution is affected by the ability of the processing algorithm to precisely determine the location of the cross correlation peak. The system vendors typically report displacement resolution error on the order of 1/20 to 1/10 of a pixel, depending on the peak finding algorithm used to process the image data. However, this minimum uncertainty is dependent on the quality of the particle images (geometry, uniformity and brightness), particle image size (pixels), the number of the particles in the IR (particle density), out-of-plane particle motion between laser pulses, and details of analysis algorithm used. These factors typically increase displacement uncertainty above that often stated by the PIV manufacture and can vary across test installations.

6.3.3 Contribution of Peak locking to Displacement Uncertainty

Another contribution to displacement uncertainty arises in biasing peak location estimation. This peak locking bias pulls displacement estimates toward integer pixel values in the correlation map displacement space. For example, it is observed in some cases that displacement estimates obtained for a uniform sub-pixel displacement of 0.5 pixels and 0.5 pixels in the X and Y directions, respectively, show the greatest amount of scatter, compared to other uniform sub-pixel displacements. This displacement error is due to the tendency of the four integer corners to pull the displacement estimates away from the input displacement at the center of the pixel array of the correlation map, as shown in Figure 44. Studies have shown that this peak locking bias error is a function of the sub-pixel particle displacement and particle image size. A small sub-pixel displacement (<0.3 pixels) can be preferentially pulled toward one pixel, while a large sub-pixel displacement (>0.7) can lock the displacement to the next pixel. This effect can have a significant impact on both the mean velocity and higher order statistics.

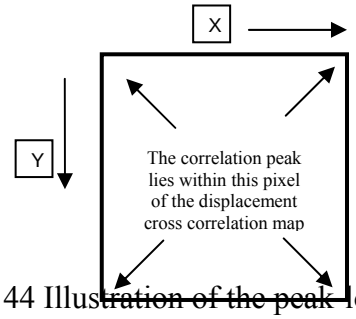

Figure 44 Illustration of the peak locking effect

A general guideline suggests that particle image sizes of at least 2 pixels and less than 10 pixels (Foucaut *et al*., 2003) can minimize peak locking. However, it is not always possible to control particle image size due to other constraints on image field-of-view (FOV), magnification, and particle size needed to accurately follow the fluid motion. As a result, the impact of peak locking on displacement uncertainty must be assessed. Particle density has been shown to impact bias and RMS displacement errors (Foucaut *et al*., 2003; Raffel *et al*., 1998; Gui and Wereley, 2002). High particle densities (>10) can significantly reduce RMS error. However, peak locking bias errors can increase with increasing particle density and densities of ~ 5 per IR are recommended in the event peak locking bias is a concern.

Investigators have used computer generated synthetic particle images to assess displacement accuracy. The EUROPIV Synthetic Image Generator is a sophisticated generator capable of simulating particle size, seeding density and image intensity. An alternative approach that has been found to work well in quantifying these affects on the displacement uncertainty including the impact of peak locking is to use images acquired during testing to digitally create image pairs with known displacements. This procedure involves generating a pseudo image pair using a MATLAB-based image processing code to displace an acquired image A to a specified displaced location B. This displaced pseudo image B is then analyzed using the PIV processing algorithms used to reduce the data. This procedure includes any affects of the camera and imaging optics, the particle seed and seed density, and the illumination and window distortions (if any). The seed and illumination aspects coupled with the camera response are believed to be critical to the applicability of the results to the experiment. Not included in this pseudo image pair approach are the effects of out-of-plane particle motion and flow gradients. These are factors the can affect the quality of the correlations but are spatial resolution and flow related bias issues and not specific to the correlation algorithms peak finding accuracy.

To assess the contribution of peak locking to both bias and random uncertainty, pseudo image pairs are created over a range of uniform sub-pixel displacements. For each pseudo image pair, the local error between the uniform displacement and the displacement engine estimate is computed, forming a displacement error ensemble for each sub pixel displacement. Performing this analysis over a range of uniform sub-pixel displacements provides a peak locking bias error sensitivity to sub-pixel displacement, allowing for a more general definition of this bias error. This technique also provides the spatial distribution of this error over the 2-D image plane where variations in laser light intensity or image distortion (like barrel distortion or window effects) may impact the magnitude of this bias. This technique does not account for intensity variations between the two laser pulses.

The scatter in the displacement estimates in the pseudo image pair results yields an estimate on the precision error. The size of the interval containing 95% of the estimated displacements, D_{95}, indicates that free of any bias error, a displacement estimate will lie within D_{95} pixels of the true value 95% of the time. The relative significance of the displacement uncertainty is a function of the velocity, the time between laser pulses and the magnification. This is unlike the magnification uncertainty which is a fixed percentage of the velocity regardless of

these factors. For example, with a defined velocity and ΔT, the precision displacement uncertainty is larger at a lower M than at a higher M where the measured Δs_i is larger with the higher M then at the lower M.

The scatter in the displacement estimates arises from noise distorted by peak locking bias. The measured pixel displacement (velocity) RMS is related to this noise contaminated measured value and the true RMS as follows:

$$RMS_{MEASURED}^2 - RMS_{NOISE}^2 = RMS_{TRUE}^2$$

In a high turbulence region, such as in a jet or wake, the noise contamination bias of the RMS is fairly inconsequential, but this error can be relatively large at lower turbulence levels. Cases in which the displacements due to turbulence span a range of just a few pixels on the correlation map can experience pixel locking from 16 or 30 integer nodes distributed across the data, as shown in Figure 45. In this case, the peak locking bias effect on the mean and RMS is expected to be substantially reduced as these influences should average out. This assessment of underlying noise establishes the noise floor of the system, including imaging, seed and processing below which turbulence levels cannot be measured. It should be noted that other factors such as spatial resolution and peak locking can and do have a large impact on the RMS estimates.

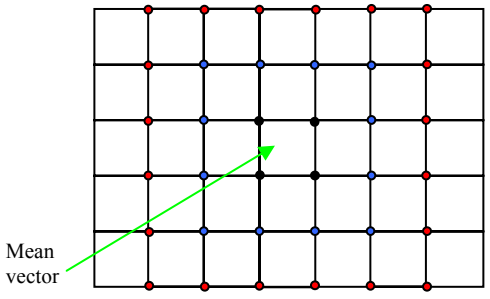

Figure 45 The number of integer displacements influencing the data increases quickly as the data distribution expands beyond one pixel.

Estimating a combined uncertainty due to the bias and scatter in the displacements observed in the pseudo image pair results, assuming a standard error propagation approach, is not valid in all cases. There are two issues. First, the bias and the scatter could be coupled. Second, the results show that the peak locking bias can act systematically and the influence of peak locking is not random such that it will average out or diminish with increased sample size. However, the direction of peak locking bias in either velocity component can be positive or negative and the bias can be a random factor that averages out under the right circumstances.

Propagating bias and scatter using values from the pseudo image analysis is appropriate in high turbulence regions, but should be done with care in low turbulence regions. If the majority of the particle displacements at one location in the flow deviate from the mean displacement by only a small amount, low turbulence, such that the data fall inside of 1 pixel on the correlation map, peak locking bias effects will be severe. In this case, the effects of peak locking do not average out because it repeats on average very well in the data. The result is the possible bias expected in the mean value is as large as the largest possible bias seen in the pseudo image analysis. These two limiting cases can be termed low pixel level turbulence and high pixel level turbulence. In high pixel level turbulence, 16 or more integer displacement nodes can influence the results and peak locking affects are expected to average out.

A common sign of peak locking bias in a vector map is the banding or segmenting of the velocity statistics around pixel displacement values. The probability density function (PDF) of the sub-pixel displacement field will show preferential grouping at integer pixel displacements instead of a relatively flat distribution. The level of peak locking can be estimated by calculating the center of mass of the sub-pixel displacement PDF and then applying the following equation:

$PL=4*(0.25-PDF_{CenterofMass})$ (Lavision, Inc)

A PL value of 0 implies no peak locking. A value of PL=1 indicates strong peak locking. Peak locking is considered to be relatively weak for PL<0.1. A regular mosaic pattern in the vorticity field computed from the velocity field can also be an indication of peak locking.

The pseudo image pair results can provide some guidance regarding the influence of peak locking on the RMS for low pixel turbulence cases. The scatter in the pseudo image pair results due to the precision with which the correlation peak can be located is much like the scatter in the displacements that would result from low levels of turbulence. A specified displacement at the center of the sub-pixel displacement results in an increase in the RMS of the data scatter compared to the mean RMS values for all the displacements considered. Displacements near integer locations should reduce calculated RMS levels due to peak locking.

6.3.4 Contribution of Perspective Distortion Bias to Displacement Uncertainty

Perspective effects can also bias the particle displacement estimates. The section on particle displacement uncertainty above considers only those sources due to the image analysis, not significant distortion of the images. This distortion bias is due to a combination of the change in the viewing angle over the FOV and the thickness of the light sheet. A particle moving from one side of the laser light sheet to the other side between laser pulses with no displacement in the plane of the laser sheet will appear to the camera to have moved in the X and/or Y directions due to perspective effects even though $\Delta X=\Delta Y = 0$. This error is smaller on the axis of the camera or near the center of the FOV due to the smaller receiving collection angle.

In practice, particles at the edges of the light sheet will not be visible and PIV data is weighted toward brighter particles that are nearer to the center of the light sheet. Displacements normal to the light sheet larger than half the sheet thickness should lead to dropouts a large fraction of the time and it is reasonable to assume the maximum perspective effects are about 2X less than the estimates made above using the full light sheet width. Raffel *et al*. (1998) provide a summary of this error. Perspective bias adds a false displacement as seen by the camera when it occurs (away from the center of the FOV). However, the sign of the displacement depends on whether the flow is moving in +Z or –Z normal to the light sheet plane. This out-of-plane motion can be expected to be random with a zero mean and no skew if the flow is symmetric about the light sheet. In this case, the bias in the mean velocity will be zero. The bias will make some velocity fluctuations seem larger than they actually were and the RMS values will be biased high as a result. However, rigorously quantifying these affects on the RMS is difficult.

6.3.5 Contribution of Spatial Resolution to Displacement Uncertainty

The spatial resolution of displacement estimate fields is defined by the size of the interrogation region (IR). Low-pass spatial filtering of the estimated velocity field can occur if the local length scale of the velocity gradients is smaller than the IR size. It is difficult to assess the impact of poor spatial resolution on displacement uncertainty since this impact is dependent on the particle density, flow gradient scale relative to the IR size, and degree of particle spatial homogeneity. A spatially inhomogeneous particle distribution across the IR, or the grouping of particles in a high speed gradient relative to a low speed gradient, can impose a velocity bias in the estimated statistical displacement over the IR. Furthermore, small gradients can impact peak locking bias and RMS. Very small gradients relative to the IR size can have minimal impact

on bias and RMS. However, as the gradient increases in scale, yet still smaller than the size of the IR, bias and RMS error increase.

6.3.6 Stereo PIV (SPIV) Uncertainty

An uncertainty procedure for SPIV would for the most part follow a similar process as defined for planar PIV. The calibration procedure is more complex in SPIV requiring either a multi-plane target or multiple target images with a target displacement. As a result, the estimation of calibration uncertainty can be more involved. Several researchers have been developing calibration techniques focused on reducing calibration error and eliminating the need for a target (Raffel *et al.*, 1998; Gui and Wereley, 2002; LaVision, Inc, Grizzi *et al.*, 2010). The dual camera setup will, however, reduce the effect of the perspective error described in section 6.3.4 (Prasad and Adrian, 1993). In addition, the "averaging" effect of the two cameras in computing the two in-plane velocity components will in general reduce the statistical uncertainty in these components. The estimation of the uncertainty in the out-of-plane component can be obtained by performing error propagation on stereo-imaging reconstruction equations used to compute the third velocity component. Prasad (2000) provides a detailed discussion on the SPIV technique. Lawson and Wu (1997a and 1997b) provide a guideline for estimating SPIV error. The third component out-of-plane error can be reduced to slightly higher than the uncertainty in the in-plane components but is typically on the order of 2 to 4 times the in-plane error.

Peak locking will also impact the overall uncertainty in SPIV if it occurs. In a similar fashion to the image displacement technique described above for planar PIV, Elbing *et al.* (2011) are developing a dual camera SPIV 3-axis image-displacement technique to estimate SPIV uncertainty and the impact of peak locking.

6.4 CFD Validation Process and Existence of Experimental Database

Despite significant progress in recent years (ITTC procedure 7.5-03-01-01), the process to perform validation of numerical simulations continues to be an active area of research and development. Many practical issues remain such as the generation of multiple systematic grids for grid refinement studies, especially when unstructured, overlapping, or adaptive grids are used to solve complex problems (moving appendages, torpedo launch, two vessels operating in close proximity, etc). In addition, as numerical simulations are required to solve more complex problems, the requirements for experimental measurements become significantly more demanding, with ever-increasing focus on unsteady nonlinear phenomena. It is not uncommon to find that existing database that had been successfully used to validate steady RANS or other more traditional numerical methods are no longer adequate to validate more advanced simulations such as URANS or LES for complex unsteady problems.

Clear needs exist to continue the assessment of the CFD validation process and to identify or develop appropriate experimental database for such a purpose.

7. CONCLUSIONS

Continued and rapid advancement in non-intrusive measurement technologies in the last 15 years has allowed researchers across many ship hydrodynamic disciplines to investigate complex and viscous phenomena involving massively separated flow and large unsteady vortical structures. This development has occurred in parallel and in conjunction with increasing usage and improvement in state-of-the-art numerical tools such as unsteady RANS and inviscid flow codes with advanced physics-based models. Nevertheless, many challenges and practical issues remain before tools such as PIV and stereo-PIV can find routine everyday

use within the towing tank community. Given the recent trend, it is expected that these technologies will continue to mature, leading to increasing adoption by the ITTC organizations.

Therefore, it is of critical importance that the ITTC addresses these practical issues and challenges in a systematic manner in order to facilitate the adoption of detailed flow measurement techniques within its member organizations.

8. RECOMMENDATIONS

The committee recommends that the ITTC:

1. Recognize the need for organized efforts to advance the application of detailed flow measurements in the ITTC community through:

- The assessment of the state of practice of detailed flow measurements within the ITTC community.
- The development of best-practice guideline on PIV/SPIV applications.
- The development of experimental benchmarks for the verification of PIV/SPIV setup.
- Continued development and assessment of uncertainty analysis procedures for PIV/SPIV, and the definition of technical standards and certification requirements.
- The evaluation of the use of flow measurements in the validation of CFD and the refinement of the process and procedure for such use.

2. Recommendation for ITTC Committees

- That the Specialist Committee on Detailed Flow Measurements develops a member survey focusing on the state of practice of flow measurement techniques within the ITTC community.
- That the Specialist Committee on Detailed Flow Measurements develops a best-practice guideline for the applications of PIV/SPIV in tow tanks and cavitation tunnels.
- That the Specialist Committee on Detailed Flow Measurements develops experimental benchmarks for the verification of PIV/SPIV setup.
- That the Specialist Committee on Detailed Flow Measurements collaborates with the Specialist Committee on Uncertainty Analysis to assess PIV error sources beyond those considered in existing procedure 7.5-01-03-03, including peak locking bias, errors due to out-of-plane velocity, effects of in-plane velocity gradients in the interrogation region, etc.
- That the Specialist Committee on Detailed Flow Measurements collaborates with the Specialist Committee on Uncertainty Analysis to develop Recommended Procedures and Guidelines on stereo-PIV uncertainty analysis.
- That the Specialist Committee on Detailed Flow Measurements collaborates with the Specialist Committee on CFD in Marine Hydrodynamics to review existing data sets suitable for benchmarking and validating CFD codes and advance the process and procedure for such use.

9. REFERENCES

Abe, M., Yoshida, N., Hishida, K., and Maeda, M., 1998, “Multilayer PIV Technique with High Power Pulse Laser Diodes,” 9th

International Symposium, Applied Laser Technology Fluid Mechanics, Lisbon, Portugal.

Alessandrini, B. and Delhommeau, G., 1998, "Viscous Free Surface Flow Past a Ship in Drift and in Rotating Motion," 22nd Symposium on Naval Hydrodynamics, Washington DC, USA.

Ando, J., Yamamoto, T., Maita, S., and Nakatake, K., 1997, "An Estimation of Hydrodynamic Forces Acting on a Ship in Oblique Towing by a Simple Surface Panel Method (SQCM)," (in Japanese), TWCNA, No. 94, pp. 13-20.

Anschau, P. and Mach, K.P., 2009, "Stereoscopic PIV Measurements of Rudder Flow and Vortex Systems in the Towing Tank," AMT'09, Nantes, France.

Arndt, R. E. A. and Dugué, C., 1992, "Recent Advances in Tip Vortex Cavitation Research," International Symposium on Cavitation and Propulsors, Hamburg.

Atlar, M., Wang, D., and Glover, E.J., 2007, "Experimental investigation into the Impact of the Slipstream Wash of a Podded Propulsor," Institutions of Mechanical Engineers: J. of Engineering for the Maritime Environment, Vol. 221 Part M.

Atsavapranee, P., Forlini, T., Furey, D., Hamilton, J., Percival, S., and Sung, C., H., 2004, "Experiment Measurements for CFD Validation of the Flow About a Submarine Model (ONR Body-1)," 25th Symposium on Naval Hydrodynamics, St. John's, Canada.

Atsavapranee, P., Carneal, J. B., Baumann, C. W., Hamilton, J. H., and Shan, J. W., 2005, "Global Laser Rangefinder Profilometry (GLRP): A Novel Optical Surface-Wave Measurement System," Naval Surface Warfare Center Carderock Division Hydromechanics Directorate Technical Report, NSWCCD-50-TR-2005/022.

Atsavapranee, P., Engle, A., Grant, D. J., Carneal, J. B., Beirne, T., Etebari, A., Percival, S., Rosario, J., Lugni, C., and Massimo, S., 2008, "Full-Scale Investigation of Viscous Roll Damping with Particle Image Velocimetry," 27th Symposium on Naval Hydrodynamics, Seoul, Korea.

Atsavapranee, P., Miller, R., Dai, C., Klamo, J., and Fry, D., 2010, "Steady-Turning Experiments and RANS Simulations on a Surface Combatant Hull Form (Model #5617)," 28th Symposium on Naval Hydrodynamics, Pasadena, USA.

Bassler, C., Lang, G., Lee, S., Carneal, J., Park, J., and Dipper, M., 2008, "Formation of Large-Amplitude Wave Groups in an Experimental Model Basin," Naval Surface Warfare Center Carderock Division Hydromechanics Directorate Technical Report, NSWCCD-50-TR-2008/025.

Billet, M., 1987, "Wake Measurements Using a Laser Doppler Velocimeter System," ITTC Symposium on Application and Accuracy of LDV Measurements.

Bishop, R., Atsavapranee, P., Percival, S., Shan, J., and Engle, A., 2004, "An Investigation of Viscous Roll Damping Through the Application of Particle-Image Velocimetry," 25th Symposium on Naval Hydrodynamics, St. John's, Canada.

Blaurock, J. and Lammers, G., 1988, "The Influence of Propeller Skew on the Velocity Field and Tip Vortex Shape in the Slipstream of Propellers," SNAME Propeller '88 Symposium, Jersey City, NJ.

Bourgoyne, D., Ceccio, S., Dowling, D., Brewer, W., Jessup, S., Park, J., and Pankajakshan, R., 2000, "Hydrofoil Turbulent Boundary Layer Separation at

High Reynolds Number," 23rd Symposium on Naval Hydrodynamics, Val de Reuil, France.

Bourgoyne, D., Hamel, J., Judge, C. Q., Ceccio, S., Dowling, and Cutbirth, J., 2002, "Hydrofoil Near-Wake Structure and Dynamics at High Reynolds Number," 24th Symposium on Naval Hydrodynamics, Fukuoka, Japan.

Bouvy, A. Henn, R. and Henβe, J., 2009, "Acoustic Wave Height Measurement in a Towing Facility," AMT'09, Nantes France, pp. 311-324.

Broglia, R., Di Mascio, A., and Muscari, R, 2004, "Numerical Simulations of Breaking Wave Around a Wedge," 25th Symposium on Naval Hydrodynamics, St. John's, Canada.

Bugalski, T., 2009, "Applications of Stereo Particle Image Velocimetry to Ship Wake and Propeller Flows," AMT'09, Nantes, France.

Bull, P., Verkuyl, J. B., Ranocchia, D., Di Mascio, A., Di Felice, F., Dattola, Cdr R., Merle, L, and Cordier, S., 2002, "Prediction of High Reynolds Number Around Navy Vessels," 24th Symposium on Naval Hydrodynamics, Fukuoka, Japan.

Van de Bunt, E. and Kaminski, M.L., 2009, "Measuring Sloshing Impacts during Full-Scale Tests," AMT '09, Nantes, France, pp. 340-355.

Calcagno, G., Di Felice, F., Felli, M., and Pereira, F., 2002, "Propeller Wake Analysis Behind a Ship by Stereo PIV," 24th Symposium on Naval Hydrodynamics, Fukuoka, Japan.

Calisal S., 2009 "A Direct Measurement of Wave Resistance by the Measurement of Wave Height on a Surface Patch," J. Ship Research, Vol. 53, No. 3, pp. 170-177.

Calisal S., Sireli, M.E., and Tan, J., 2011, "A Longitudinal Cut Method by the Measurement of Wave Height on a Surface Patch", AMT '11, Newcastle, UK pp. 367-381.

Campana, E. F., Di Mascio, A., and Penna, R., 1998, "CFD Analysis of the Flow Past a Ship in Steady Drift Motion," 3rd Osaka Colloquium on Advanced Applications to Ship Flow and Hull Form Design (OC'98), Osaka, Japan.

Carneal, J. B., Cutright, J. T., and Atsavapranee, P., 2005, "Global Laser Rangefinder Profilometry: Initial Test and Uncertainty Analysis," Naval Surface Warfare Center Carderock Division Hydromechanics Directorate Technical Report, NSWCCD-50-TR–2005/069.

Cenedese, A., 1985, "Phase Sampling in the Analysis of a Propeller Wake," International Conference on Laser Anemometry Advances and Application, Manchester, UK.

Chesnakas C. and Jessup S., 1998, "Experimental Characterisation of Propeller Tip Flow," 22nd Symposium on Naval Hydrodynamics, Washington, DC.

Chesnakas, C. J. and Jessup, S. D., 2003, "Tip-Vortex Induced Cavitation on a Ducted Propulsor," ASME Symposium on Cavitation Inception, Honolulu, USA.

Cotroni, A., Di Felice, F., Romano, G. P., Elefante, M., 2000, "Investigation of the Near Wake of a Propeller using Particle Image Velocimetry," Exp. Fluids 29, S227–S236 suppl. 476-481.

Crafton, J., Fonov, S. D., Jones, E. G., Goss, L. P., Forlines, R. A., and Fontaine, A., 2008, "Measurements of Skin Friction in Water using Surface Stress Sensitive Films," Meas. Sci. Technol., 19.

Day, A. H., Clelland, D., and Valentine, G., 2011, "Development of a Low-Cost Laser Wave Measurement System," AMT '11, Newcastle, UK pp 439-452.

Di Felice, F. and Mauro, S., 1999, "LDV Cross-Flow Survey on a Series 60 Double Model at Incidence," Proceedings of ISOPE'99, 9th International Offshore and Polar Engineering Conference, Brest, France, pp. 536-543.

Di Felice F., Del Rosso, C., and Romano G. P., 2011, "On the Formation and Evolution of the Tip and Hub Vortex of a Propeller," AMT'11, Newcastle, UK.

Di Felice F., Di Florio, D., Felli, M., Romano, G. P., 2004, "Experimental Investigation of the Propeller Wake at Different Loading Conditions by Particle Image Velocimetry," J. Ship Research, Vol. 48, pp. 168–190.

Di Felice, F. and Pereira F., 2007, "Developments and Application of PIV in Naval hydrodynamics", PIV: new developments and Recent Applications by A. Schroder, K. E. Willert, Springer-Verlag.

Dong, R. R., Katz, J., and Huang, T. T., 1997, "On the Structure of Bow Waves on a Ship Model," J. Fluid Mechanics, Vol. 346, pp. 77-115.

Drain, L. E., 1980, "The Laser Doppler Technique," John Wiley & Sons.

Elbing, B. R., Petrie, H.L., and Fontaine, A. A., 2001, "Articial Shifting of Stereo PIV Images for Uncertainty Estimation," Manuscript in process.

El-Lababidy, S., Bose, N., Pengfei, L., Di Felice, F., Felli, M., and Pereira, F., 2004, "Experimental Analysis of the Wake from a Dynamic Positioning Thruster," 25th Symposium on Naval Hydrodynamics, St. John's, Canada.

Elsinga, G. E., Scarano, F., Wieneke, B., and Van Oudheusden, B. W., 2006, "Tomographic Particle Image Velocimetry," Exp. Fluids, Vol. 41, 933-947.

Etebari, A., Atsavapranee, P., Carneal, J. B., Percival, S., Grant, D., Sung, S. H., and Koh, I. Y., 2008, "Experimental Measurements on a SUBOFF Model in a Turning Maneuver," 27th Symposium on Naval Hydrodynamics, Seoul, Korea.

Felli, M., Di Felice, F., and Lugni, C., 2004, "Experimental Study of the Flow Field Around a Rolling Ship Model," 25th Symposium on Naval Hydrodynamics, St. John's, Canada.

Felli, M., and Di Felice, F., 2005, "Propeller Wake Analysis in Nonuniform Inflow by LDV Phase Sampling Techniques," J. of Marine Science and Technology, Vol. 10, No. 4, pp.159-172.

Felli, M., Camussi, R., and Guj, G., 2009, "Experimental Analysis of the Flow Field around a Propeller-Rudder Configuration," Exp. Fluids, Vol. 46, No. 1, pp. 147-164.

Felli, M. and Di Felice, F., 2004, "Analysis of the Propeller-Hull Interaction by LDV Phase Sampling Techniques," J. of Visualization, Vol. 7, No. 1, pp. 77–84.

Felli, M., Di Felice, F., Guj, G., and Camussi, R., 2006, "Analysis of the Propeller Wake Evolution by Pressure and Velocity Phase Measurements," Exp. Fluids, Vol. 41, No. 3, pp. 441–451.

Felli, M., Greco, L., Colombo, C., Salvatore, F., Di Felice, F., and Soave, M., 2006, "Experimental and Theoretical Investigation of Propeller-Rudder Interaction Phenomena," 26th Symposium on Naval Hydrodynamics, Rome, Italy.

Felli, M., Guj, G., and Camussi, R., 2008, "Effect of the Number of Blades on

Propeller Wake Evolution," Exp. fluids, Vol. 44, No. 3, pp. 409-418.

Felli, M., Pereira, F., Calcagno, G., and Di Felice, F., 2003, "A modular Stereo-PIV Probe for Underwater Applications: Configurations and Measurement Performance," PIV'03, Busan, Korea.

Felli, M., Falchi, M., Pereira, F., and Di Felice, F., 2010, "Dynamics of the Propeller Wake Structures Interacting with a Rudder," 28th Symposium on Naval Hydrodynamics, Pasadena, USA.

Foucaut, J. M., Miliat, B., Perenne, N., and Stanislas, M., 2003, "Characterization of Different PIV Algorithms using the EUROPIV Synthetic Image Generator and Real Images From a Turbulent Boundary Layer," EUROPIV 2 Workshop, Zaragosa, Spain.

Fouras, A., Jacono, D. L., and Hourigan, K., 2008, "Target Free Strereo PIV: a Novel Technique with Inherent Error Estimation and Improved Accuracy," Exp Fluids, Vol. 44, No. 2, pp. 317-329.

Fruman, D. H., Dugué, C., Pauchet, A., Cerruti, P., and Briançon-Marjolet, L., 1992, "Tip Vortex Roll-Up and Cavitation," 19th Symposium on Naval Hydrodynammics, Seoul, Korea.

Fruman, D. H., Cerruti, P., Pichon, P., and Dupont, P., 1993, "Effect of Hydrofoil Planform on Tip Vortex Roll-up and Cavitation," ASME International Symposium on Cavitation Inception, FED-Vol. 177, pp. 113-124, New Orleans, Louisiana.

Fu, T. C., Atsavapranee, P., and Hess, D. E., 2002, "PIV Measurements of the Cross-Flow Wake of a Turning Submarine Model (ONR Body-1)," 24th Symposium on Naval Hydrodynamics, Fukuoka, Japan.

Fu, T. C., Karion, A., Pence, A., Rice, J. Walker, D., Pence, M. L., and Ratcliffe, T., 2005, "Characterization of the Steady Wave Field of the High Speed Transom Stern Ship - Model 5365 Hull Form," Naval Surface Warfare Center Carderock Division Hydromechanics Directorate Technical Report, NSWCCD-50-TR-2005/04.

Fu, T. C. and Fullerton, A., 2006, "Measurements of the Wave Field Around the *R/V Athena I*," 26th Symposium on Naval Hydrodynamics, Rome, Italy.

Fu, T. C., Fullerton, A. M., Ratcliffe, T., Minnick, L., Walker, D., Pence, M. L., and Anderson, K., 2009, "A Detailed Study of Transom Breaking Waves," Naval Surface Warfare Center Carderock Division Hydromechanics Directorate Technical Report, NSWCCD-50-TR-2009/025.

Fullerton, A. M., and Fu, T. C., 2008, "Acoustic Doppler Current Profiler (ADCP) Measurements of Breaking Waves," FEDSM2008, Jacksonville, Florida, USA.

Furey D., and Fu, T. C., 2002, "Quantitative Visualisation (QViz) Hydrodynamic Measurement Technique of Multiphase Unsteady Surfaces," 24th Symposium on Naval Hydrodynamics, Fukuoka, Japan.

Geerts, S., Van Kerkhove, G. Vantorre, M. and Delefortrie G., 2011, "Waterline Registration using Fluorescent Lighting," AMT '11, Newcastle, UK, pp 61-69.

Goss, L. P., Estevadeordal, J., Crafton, J. W., 2007a, "Velocity Measurements Near Walls, Cavities, and Model Surfaces Using Particle Shadow Velocimetry (PSV)," 22nd International Congress on Instrumentation in Aerospace Simulation Facilities (ICIASF 2007).

Goss, L. P., Estevadeordal, J., and Crafton, J. W., 2007b, "Kilo-Hertz Color Particle

Shadow Velocimetry (PSV)," AIAA-2007-4507, 37th AIAA Fluid Dynamics Conference, Miami, FL.

Grizzi, S., Pereira, F., and Di Felice, F., 2010, "A Simplified, Flow-Based Calibration Method for Stereoscopic PIV," Exp Fluids, Vol. 48, pp. 473-486.

Gui, L., Longo, J., Metcalf, B., Shao, J., and Stern, F., 2000, "Forces, Moments and Wave Pattern for Naval Combatant in Regular Head Waves," 23rd Symposium on Naval Hydrodynamics, Val de Reuil, France.

Gui L. and Wereley, S. T., 2002, "A correlation based continuous window shift technique to reduce peak locking effect on digital image evaluation, Exp. Fluids, Vol. 32, pp. 506-517.

Hallmann, R., Tukke, J., and Verhulst, M. A., 2009, "Challenges for PIV in Towing Facilities," AMT'09, Nantes, France

Hearn, G. E. and Clark, D., 1993, "Manoeuvring of Ships and Estimation Schemes (MOSES): The Influence of Vortices on the Calculation of Hull Derivative," International Conference on Marine Simulation and Ship Manoeuvrability (MARSIM'93), St John's, Canada, pp. 171-178.

Hinsch, K.D., 2002, "Holographic particle image velocimetry", Meas. Sci. Technol. Vol. 13, pp. 61–72.

Hirano, M. and Takashina, J., 1980, "A Calculation of Ship Turning Motion Taking Coupling Effect Due to Heel into Consideration," Trans. West-Japan Society of Naval Architects, Vol. 59, pp. 71-81.

Hooft, J. P., 1994, "The Cross-Flow Drag on a Manoeuvring Ship," Ocean Engineering, Vol. 21, No. 3, pp. 329-342.

Hoshino, T. and Oshima, A, 1987, "Measurement of the Flow Field Around a Propeller by using a 3-Component Laser–Doppler Velocimeter", Mitsubishi Technical Review, No. 24.

Hoshino, T, 1989, "Hydrodynamic Analysis of Propellers in Steady Flow using a Surface Panel Method", Journal of the Society of Naval Architects of Japan, Vol. 165, pp.55-70.

Hoshino, T, 1990, "Numerical and Experimental Analysis of Propeller Wake by using Surface Panel Method and a 3-Component LDV", 18th Symposium on Naval Hydrodynamics, Ann Arbor, Michigan.

Hudy, L. M. and Naguib, A. M, 2003, "Wall-Pressure-Array Measurements Beneath a Separating/Reattaching Flow Region," Phys. Fluids, Vol. 15, No. 3, pp. 706-717.

Irvine, M., Longo, J., and Stern, F., 2004, "Towing-Tank Tests for Surface Combatant for Free Roll Decay and Coupled Pitch and Heave Motions," 25th Symposium on Naval Hydrodynamics, St. John's, Canada.

Jessup, S., Chesnakas, C., Fry, D., Donnelly, M., Black S., and Park, J., 2004, "Propeller Performance at Extreme Off Design Conditions", 25th Symposium on Naval Hydrodynamics, St. John's, Canada.

Jessup, S., Fry, D., and Donnelly, M., 2006, "Unsteady Propeller Performance in Crashback Conditions with and without a Duct", 26th Symposium on Naval Hydrodynamics, Rome, Italy.

Jessup, S. D., 1989, "An Experimental Investigation of Viscous Aspects of Propeller Blade Flow", PhD thesis, Catholic University of America, Washington DC.

Jessup, S. D., 2008, "Performance Analysis of a Four Waterjet Propulsion System for a Large Sealift Ship", 27th Symposium on Naval Hydrodynamics, Seoul, Korea.

Jessup, S. D., Schott, C., Jeffers, M., and Kobayashi, S., 1985, "Local Propeller Blade Flows in Uniform and Sheared Onset Flows using LDV Techniques," 15th Symposium on Naval Hydrodynamics, Hamburg, Germany.

Jiang, C. W., Dong, R. R, Liu, H. L., and Chang, M. S., 1996, "24-inch Water Tunnel Flow Field Measurements During Propeller Crashback," 21st Symposium on Naval Hydrodynamics, Trondheim, Norway.

Kähler, C. J. and Kompenhans, J., 2000, "Fundamentals of Multiple Plane Stereo Particle Image Velocimetry," Exp. Fluids, Vol. 29.

Kajima, K. and Tanaka, S., 1992, "The Cross Flow Drag Acting on Rectangular Cross Sections With Round Edge," (in Japanese) Journal of the Society of Naval Architects of Japan, Vol. 172, pp. 1-8.

Kakugawa, A. and Takei, Y., 1986, "Measurement of Boundary Layer on a Propeller Blade using LDV Technique," J. KSNAJ, Vol. 203, pp 21-25

Kaminski, M. L. and Bogaert, H., 2009, "Full Scale Sloshing Impact Tests," 19th International Offshore and Polar Engineering Conference (ISOPE), Osaka, Japan.

Kanai, M., 1985, "Wave Analysis by Grid Projection Method," Journal of the Society of Naval Architects of Japan, Vol. 193, pp. 127-135.

Katz, J., Gowing, S., O'Hern, T., and Acosta, A., 1983, "A Comparative Study Between Holographic and Light-Scattering Techniques of Microbubble Detection," Proc. Symposium, Measuring Techniques in Gas-Liquid Two-Phase Flows, Nancy, France.

Kerwin, J. E.,1982, "Flow Field Computation for Non-Cavitating and Cavitating Propellers", 14th symposium on Naval Hydrodynamics, Ann Arbor, Michigan.

Kijima, K., Yukawa, K., and Maekawa, K, 1995, "An Estimation of Hydrodynamic Forces Acting on a Ship Hull in Oblique Motion," (in Japanese), TWSNA, No. 90, pp. 115-125.

Kijima, K., Yukawa, K., and Maekawa, K, 1996, "An Estimation of Hydrodynamic Forces Acting on a Ship Hull in Oblique Motion (continued)," (in Japanese), TWSNA, No. 91, pp. 95-106.

Kobayashi, S., 1981, "Experimental Methods for the Prediction of the Effect of Viscosity on Propeller Performance,". MIT department of Ocean Engineering, Report 81-7.

Kobayashi, S. and Bugenhagen, K., 1981, "Viscous Flow on and Around Propeller Blades," ORI Technical Report, N. TR 2451.

Kose, K., Misiag, W. A., Zhu, J., and Hirao, S., 1992, "Databse System Approach for Maneuvering Performance Prediction," Journal of the Society of Naval Architects of Japan, Vol. 172, pp. 375-382.

LaVision, Inc.

Lawson, N. and Wu, J., 1997a, "Three-Dimensional Particle Image Velocimetry: Error Analysis of Stereoscopic Techniques," Meas. Sci. Tech., Vol. 8, pp. 894-900.

Lawson, N. and Wu, J., 1997b, "Three-Dimensional Particle Image Velocimetry: Experimental Error Analysis of a Digital

Angular Stereoscopic System," Meas. Sci. Tech., Vol. 8, pp. 1455-1464.

Lee S. J., Paik B. G., and Lee C.M., 2002, "Phase-averaged PTV Measurements of Propeller Wake", 24th Symposium on Naval Hydrodynamics, Fukuoka, Japan.

Liefvendal, M., Felli, M., and Troeng, C., 2010, "Investigation of Wake Dynamics of a Submarine Propeller", 28th Symposium on Naval Hydrodynamics, Pasadena, USA.

Liu, H., L, and Fu, T., 1994, "PDV Measurement of Vortical Structures in the DTMB Rotating Arm Facility," DTMB Report CRDKNSWC/HD-1416-02.

Longo, J., Huang, H.P., and Stern, F., 1998, "Solid/free-surface Juncture Boundary Layer and Wake," Exp. Fluids, Vol. 25, pp. 283-297.

Longo, J. and Stern, F., 1996, "Yaw Effects on Model-Scale Ship Flow," 21st Symposium on Naval Hydrodynamics, Trondheim, Norway.

Lubke, L. O. and Mach, K. P., 2004, "LDV Measurements in the Wake of the Propellerd KCS Model and its Use to Validate CFD Valculation," 24th Symposium on Naval Hydrodynamics, St John's, Canada.

Lurie, E. H., 1993, "Unsteady Response of a Two Dimensional Hydrofoil Subject to High Reduced Frequency Gust Loading," MIT Report, 93-5.

Maas, H. G., Gruen, A., and Papantoniou D., 1993, "Particle Tracking Velocimetry in Three-Dimensional Flows: Part 1. Photogrammetric Determination of Particle Coordinates," Exp. Fluids, Vol. 15, No. 2, pp. 133-146.

Martins, J. A. de A., de Mello, P. C., Carneiro, M. L., Souza, C. A. G. F., and Adamowski, J. C., 2007, "Laboratory Wave Probes Dynamic Performance Evaluation," Proc. XX COPINAVAL - Congresso PanAmericano de Engenharia Naval e Transportes Marítimos, São Paulo, Brazil.

Martinsen R. J., and Bock., E. J., 1992, "Optical Measurements of Ripples using a Scanning-Laser Slope Gauge: Part I - Instrumentation and Preliminary Results," Proc. Int. Soc. for Optical Engineering, Vol. 1749, pp. 258–271, San Diego, CA, USA.

McPhail, M. Giordano, J., Fontaine, A., Krane, M., Goss, L. and Crafton, J., 2010, "Particle Shadow Velocimetry vs LDV: Measurements of a Turbulent Pipe Flow," MW.00004, 63rd Annual meeting of the APS Div. Fluid Dynamics, Vol. 55, No. 6, Long Beach, CA.

Michael, T. J. and Chesnakas, C. J., 2004, "Advanced Design, Analysis, and Testing of Waterjet Pumps," 25th Symposium on Naval Hydrodynamics, St. John's, Canada.

Miller, R. W., Bassler, C. C., Atsavapranee, P., Gorski, J. J., 2008, "Viscous Roll Predictions for Naval Surfacce Ship Appended with Bilge Keels using URANS," 27th Symposium on Naval Hydrodynamics, Seoul, Korea.

Min, K. S., 1978, "Numerical and Experimental Methods for Prediction of Field Point Velocities Around Propeller Blades," MIT Department of Ocean Engineering, Report 78-12.

Miorini, R. L., Wu, H., Tan, D., and Katz, J., 2010, "Flow Structures and Turbulence in the Rotor Passage of an Axial Waterjet Pump at Off-Design Conditions," 28th Symposium on Naval Hydrodynamics, Pasadena, USA.

Mukto, M. A., Atmane, M. A., and Loewen, M. R., 2007, "A Particle-Image Based Wave

Profile Measurement Technique," Exp Fluids, Vol. 42, pp. 131–142.

Muscari, R., Felli, M., and Di Mascio, A., 2010, "Numerical and Experimental Analysis of the Flow Around a Propeller Behind a Fully Appended Hull", 28th Symposium on Naval Hydrodynamics, Pasadena, USA.

Nakatake, K., Ando, J., Maita, S., and Yamamoto, T., 1998, "Prediction of Forces Acting on Ship with Different Afterbody Shapes in Oblique Towing," MAN'98, Val de Reuil, France, pp. 173-180.

Nagaya, S., Ochi, F., Fukui, Y., Omori, T., and Inukai, Y., 2011, "Stereo PIV Measurements of Flow Around Energy Saving Device and Twin-Skeg Stern Ship in Towing Tank," AMT'11, Newcastle, UK.

Nonaka, K., Nimura, T., Haraguchi, T., and Ueno, M., 1995, "Measurement of Stern Flow Field of a Ship in Olique Towing Motion," (in Japanese) Journal of the Society of Naval Architects of Japan, Vol. 177, pp. 29-40.

Ohkusu, M., 1980, "Added Resistance in Waves in the Light of Unsteady Wave Pattern Analysis," 13th Symposium on Naval Hydrodynamics, Japan.

Ohkusu, M. and Wen, G., 1996, "Radiation and Diffraction Waves of a Ship at Forward Speed," 21st Symposium on Naval Hydrodynamics, Trondheim, Norway.

Ohkusu, M. and Yasunaga, M., 2000, "Second Order Waves Generated by Ship Motions," 23rd Symposium on Naval Hydrodynamics, Val de Reuil, France.

Ohmori, T. and Miyata, H., 1993, "Oblique Tow Simulation by a Finite-Volume Method," Journal of the Society of Naval Architects of Japan, Vol. 173, pp. 27-34.

Ohmori, T., Fujino, M., Miyata, H., and Kanai, M., 1994, "A Study on Flow Field Around Full Ship Forms in Maneuvering Motion (1st Report: In Oblique Tow)," (in Japanese) Journal of the Society of Naval Architects of Japan, Vol. 176, pp. 241-250.

Oshima, A., 1994, "Study of Tip Vortex Cavitation Inception of Propeller", 2nd International Symposium on Cavitation, Tokyo, Japan.

Paik B. G., Lee C. M., Lee S. J., 2005, "Comparative Measurement on Flow Structure of Marine Propeller Wake Between Open Free Surface and Closed Surface Flows", J. of Marine Science and Technology, Vol. 10, pp. 123–130.

Paik, B. G., Kim, J., Park, Y. H., Kim, K. S., and Yu, K. K., 2007, "Analysis of Wake Behind a Rotating Propeller using PIV Technique in a Cavitation Tunnel", J. of Ocean Engineering, Vol. 34, Issues 3-4.

Pauchet, A., 1996, "Velocity and Turbulence in the Near Field Region of Tip Vortices from Elliptical Wings. Its Impact on Cavitation," 21st Symposium on Naval Hydrodynamics, Trondheim, Sweden.

Payne G., Richon J-B, Ingram D., Spinneken J., 2009, "Development and Preliminary Assessment of an Optical Wave Gauge," 8th European Wave and Tidal Energy Conference (EWTEC 2009), Uppsala, Sweden.

Pereira, F., Gharib, M., 2004, "A Method for Three-Dimensional Particle Sizing in Two-Phase Flows," Measurement in Science and Technology, Vol. 15, 2029–2038.

Pereira, F., Castaño-Graff, E., Gharib, M., 2006, "Bubble Interaction with a Propeller Flow," 26th Symposium on Naval Hydrodynamics, Rome, Italy.

Pereira, F., 2011, "Transport of Gas Nuclei in a Propeller Flow," SMP'11, Hamburg, Germany.

Perelman, O., Wu, C. H. Boucheron R., Fréchou D., 2011, "3D Wave Fields Measurement Techniques in Model Basins: Application on Ship Wave Measurement," AMT '11, Newcastle, UK.

Prasad, A. K. and Adrian, R. J., 1993, "Stereoscopic Particle Image Velocimetry Applied to Liquid Flows," Exp. Fluids, Vol. 15, pp. 49-60.

Prasad, K., 2000, "Stereoscopic Particle Image Velocimetry," Exp. Fluids, Vol. 29, pp. 103-116.

Pu, Y. and Meng, H., 2000, "An Sdvanced Off-Axis Holographic Particle Image Velocimetry System," Exp. Fluids, Vol. 29, pp. 184–197.

Raffel, M., Willert, C. E., Kompenhans, J., "Particle Image Velocimetry: A Practical Guide," Springer Verlag, 1998.

Ratcliffe, T., 2000, "An Experimental and Computational Study of the Effects of Propulsion on the Free-Surface Flow Astern of Model 5415," 23rd Symposium on Naval Hydrodynamics, Val de Reuil, France.

Rice, J. R., Fu, T. C., Karion, A. Walker, D. and Ratcliffe, T., 2004, "Quantitative Visualization of the Free-Surface Around Surface Ships," 25th Symposium on Naval Hydrodynamics, St Johns, Newfoundland, Canada.

Richon, J. B., Reeves, M., Darquier M. and Fréchou D., 2009, "Development of a Laser Gauge for Dynamic Wave Height Measurements in the B600 Towing Tank," AMT '09, Nantes, France.

Rood, E. P., Anthony, D. G., 1988, "An Experimental Investigation of Propeller-Hull Appendage Hydrodynamic Interaction," 17th Symposium on Naval Hydrodynamics, Hague, Netherlands.

Roth, G. I., Mascenik, D. T., and Katz, J., 1999, "Measurements of the Flow Structure and Turbulence Within a Ship Bow Wave," Phys. Fluids, Vol. 11, pp. 3512-3523.

Sanada, Y., Toda, Y., and Hamachi, S., 2008, "Free Surface Measurement by Reflected Light Image," 25th International Towing Tank Conference (ITTC), Fukuoka, Japan Vol. 3, pp 814-820.

Santiago, J. G., Wereley, S. T., Meinhart, C. D., Beebe, D. J., and R. J. Adrian, 1998, "A Particle Image Velocimetry System for Microfluidics," Exp. Fluids, Vol. 25, pp. 316-319.

Shen Y. T., Remmers K. D., and Jiang C. W., 1997, "Effect of Ship Hull and Propeller on Rudder Cavitation," J. Ship Research, Vol. 41(3), pp.172–180.

Stella A., Guj G., and Di Felice F., 2000, "Propeller Flow Field Analysis by Means of LDV Phase Sampling Techniques," Exp. Fluids, Vol. 28, pp. 1–10.

Stern, F., Longo, J., Penna, R., Olivieri, A., Ratcliffe, T., and Coleman, H., 2000, "International Collaboration on Benchmark CFD Validation Data for Surface Combatant DTMB Model 5415," 23rd Symposium on Naval Hydrodynamics, Val de Reuil, France.

Tahara, Y., 1999, "Wave Influences on Viscous Flow Around a Ship in Steady Yaw Motion," Journal of the Society of Naval Architect of Japan, Vol. 186, pp. 157-168.

Tahara, Y., Longo, J., and Stern, F., 1999, "Comparison of CFD and EFD for the Series 60 CB=0.6 in Steady Drift Motion," J. of Marine Science and Technology, Vol. 7, No. 1, pp. 17-30.

Tanaka, S, and Kajima, K., 1993, "On the Distribution of Cross Flow Drag over the Length of a Ship Moving Tranversely," (in Japanese) J. of the Society of Naval Architects of Japan, Vol. 174, pp. 357-363.

Toda, Y., Stern, F., and Longo, J., 1992, "Mean-Flow Measurements in the Boundary Layer and Wake and Wave Field of a Series 60 C_B=0.60 Ship Model," J. Ship Research, Vol. 36, No. 4, pp. 360-377.

Wanek, J. M., and Wu, C. H., 2006 "Automated Trinocular Stereo Imaging System for Three-Dimensional Surface Wave Measurements," Ocean Engineering, Vol. 33, pp 723–747.

Waniewsi, T. A., Brennen, C. E., and Raichlen, F., 2002, "Bow Wave Dynamics," J. Ship Research, Vol. 46, No. 1, pp. 1-15.

Wienef, B, 2005, "Stereo-PIV Using Self-Calibration on Particle Images," Exp. Fluids, Vol. 39, pp. 267-280.

Willert, C.E. and Gharib M., 1992, "Three-Dimensional Particle Imaging with a Single Camera," Exp. Fluids, Vol. 12, pp. 353-358.

Wu, H., Miorini, R. L., and Katz, J., 2009, "Tip Leakage Vortex Structure and Turbulence in the Meridional Plane of an Axial Pump", 8th International Symposium on Particle Image Velocimetry, Melbourne, Australia.

Yamaguchi, H., Kato, H., Takasugi, N., Shigemitsu, H., and Harada, M., 1995, "Study of Cavitation on a Finite Span Foil With Sweptback Planform," International Symposium on Cavitation, Deauville, France.

Yang CI, Jessup, SD, 1988, "Benchmark Analysis of a Series of Propellers with a Panel Method," SNAME Propeller '88 Symposium, Virginia Beach, Virginia.

Yao, A., and Wu, C. H., 2005 "An Automated Image-Based Technique for Tracking Sequential Surface Wave Profiles," Ocean Engineering, Vol. 32, pp. 157–173.